Supporting Information

1. Experimental part

1.1. General informations

^{1}H and ^{19}F NMR experiments have been recorded at respectively 600 and 565 MHz, using standard 5 mm NMR tubes. CD_2Cl_2 was stored over K_2CO_3, otherwise filtered over a short column of basic alumina before use. For low temperature NMR experiments, the sample was allowed to stand in the magnet at the desired temperature for at least 10 min before recording. Chemical shifts are expressed in parts per million (abbreviations for multiplicities and descriptors are s = singlet [s_b = broad singlet, and so on], d = doublet, t = triplet, m = multiplet, dd = doublet of doublets, dt = doublet of triplets, and br = broad signal) and coupling constants are given in Hz. Traces of residual protonated solvents were used as internal standards. **[26]HCD** and **[28]HCD** have been prepared as previously described.[1] CH_2Cl_2 was distilled over CaH_2. Commercial products were used as received.

1.2. Typical procedure for a ^{1}H NMR titration experiment of **[26]HCD** with MSA

4 mg (1.10 µmol) of **[26]HCD** were dissolved in 500 µL of CD_2Cl_2, and a ^{1}H NMR spectrum was recorded at 223 K. A solution of MSA (1.8 µL, 27.5 µmol) in CD_2Cl_2 (1 mL) was used for the titration up to 4 equiv. of acid (10 µL = 0.25 equiv.). For higher amounts of acid, pure MSA was used (0.5 µL = 8 equiv.).

1.3. Typical procedure for a UV-vis titration experiment of **[26]HCD** with MSA

10 mg (2.74 µmol) of **[26]HCD** were dissolved into 5.5 mL of distilled CH_2Cl_2 (solution L1), and 50 µL of this solution were diluted with CH_2Cl_2 to reach a total volume of 5 mL, affording a 5 µM solution used for the UV-vis titration experiments (solution L2). Three different solutions of MSA were prepared (S1, S2 and S3) by dissolving 5 µL of the acid into respectively 1 mL (S1), 10 mL (S2) and 40 mL (S3) of CH_2Cl_2. For 1.5 mL of L2, 1 µL of these solutions (S1-S3) corresponds respectively to 10, 1, and 0.25 equivalents of MSA.

[1] M. Ménand, M. Sollogoub, B. Boitrel and S. Le Gac, *Angew. Chem. Int. Ed.,* 2016, **55**, 297.

2. UV-vis titration experiments

2.1. Titration of **[26]HCD** with TFA (a-b) and MSA (c-e)

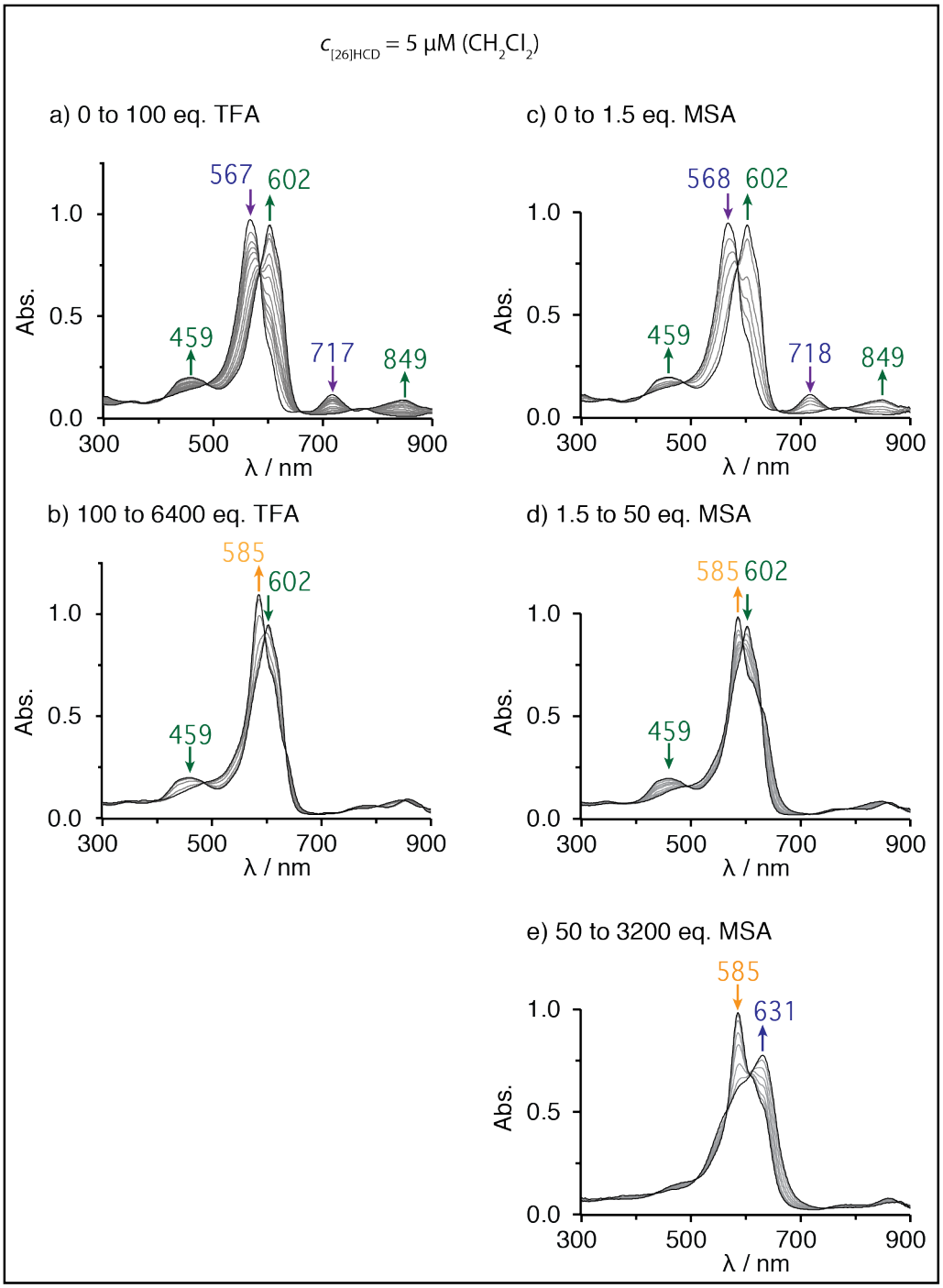

2.2. Titration of **[28]HCD** with TFA (a-c) and MSA (d-f)

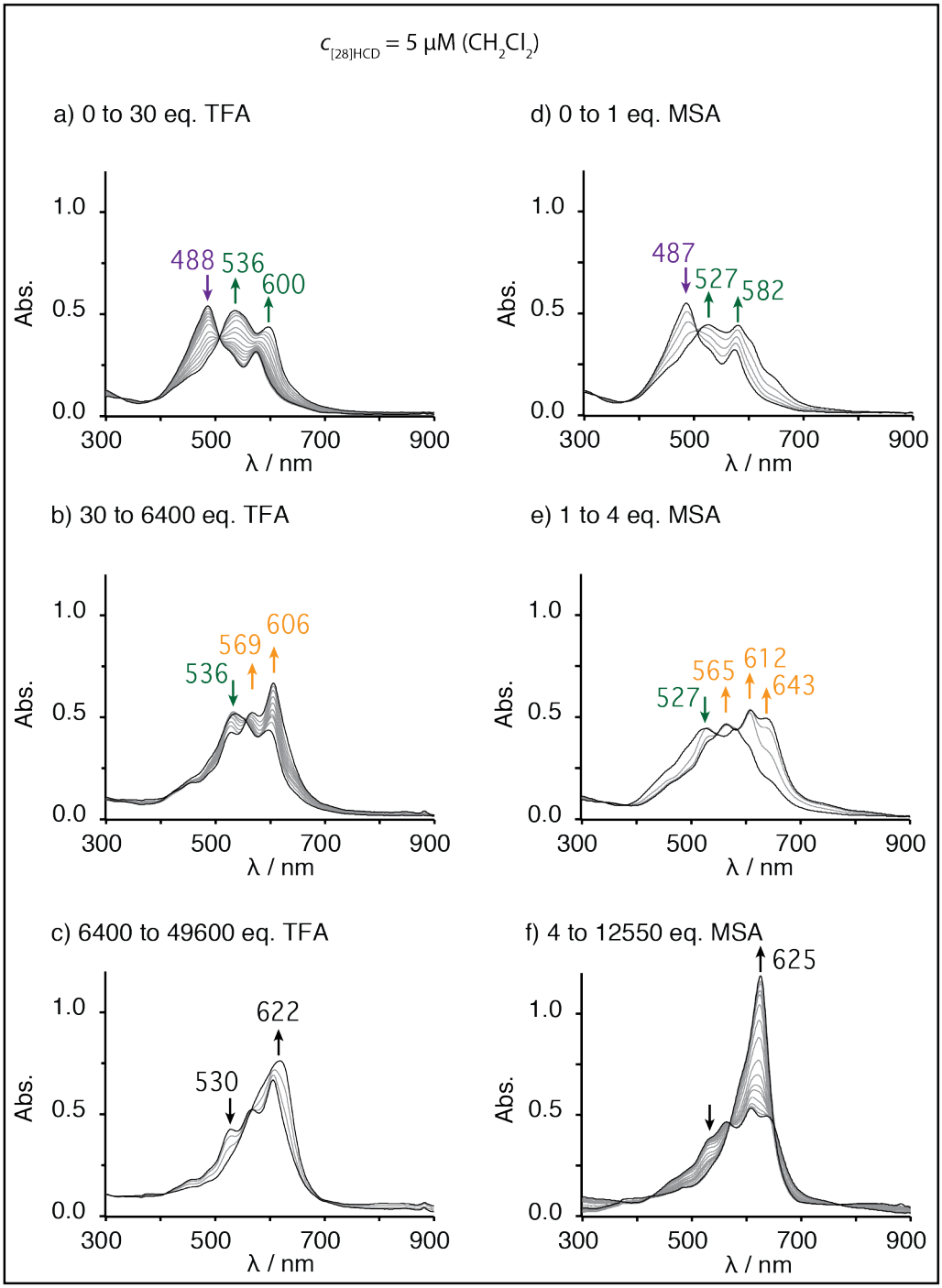

3. ^{1}H NMR titration experiments

3.1. Titration of **[26]HCD** with MSA (600 MHz, CD_2Cl_2, 223 K)

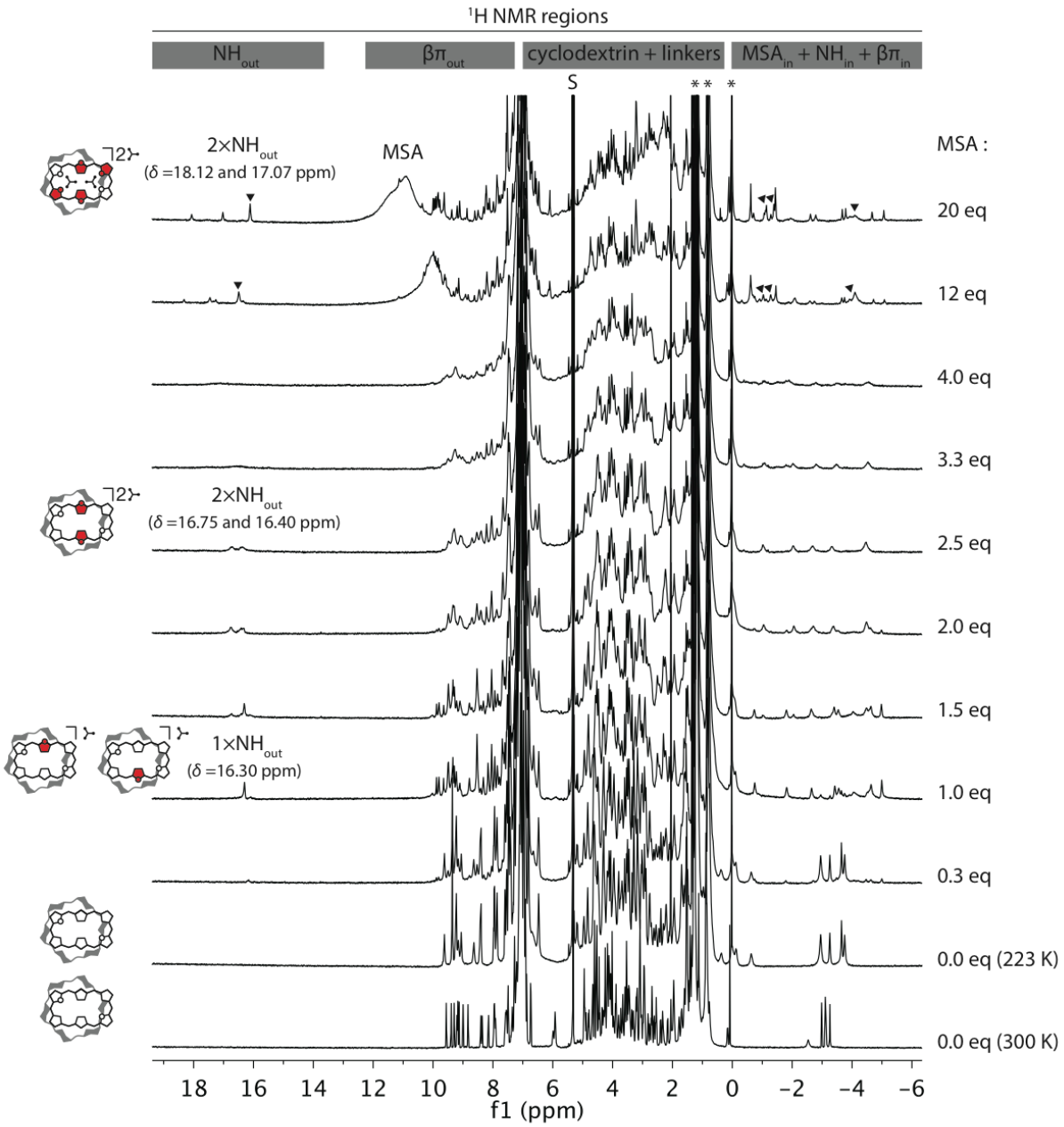

S: solvent, ▼: ^{T}**[26]HCD•4H^{+}⊃MSA^{-}** contamination and *: impurities.

3.2. Titration of **[26]HCD** with MSA (600 MHz, CD_2Cl_2, 223 K) – zoom on the βπ/NH regions

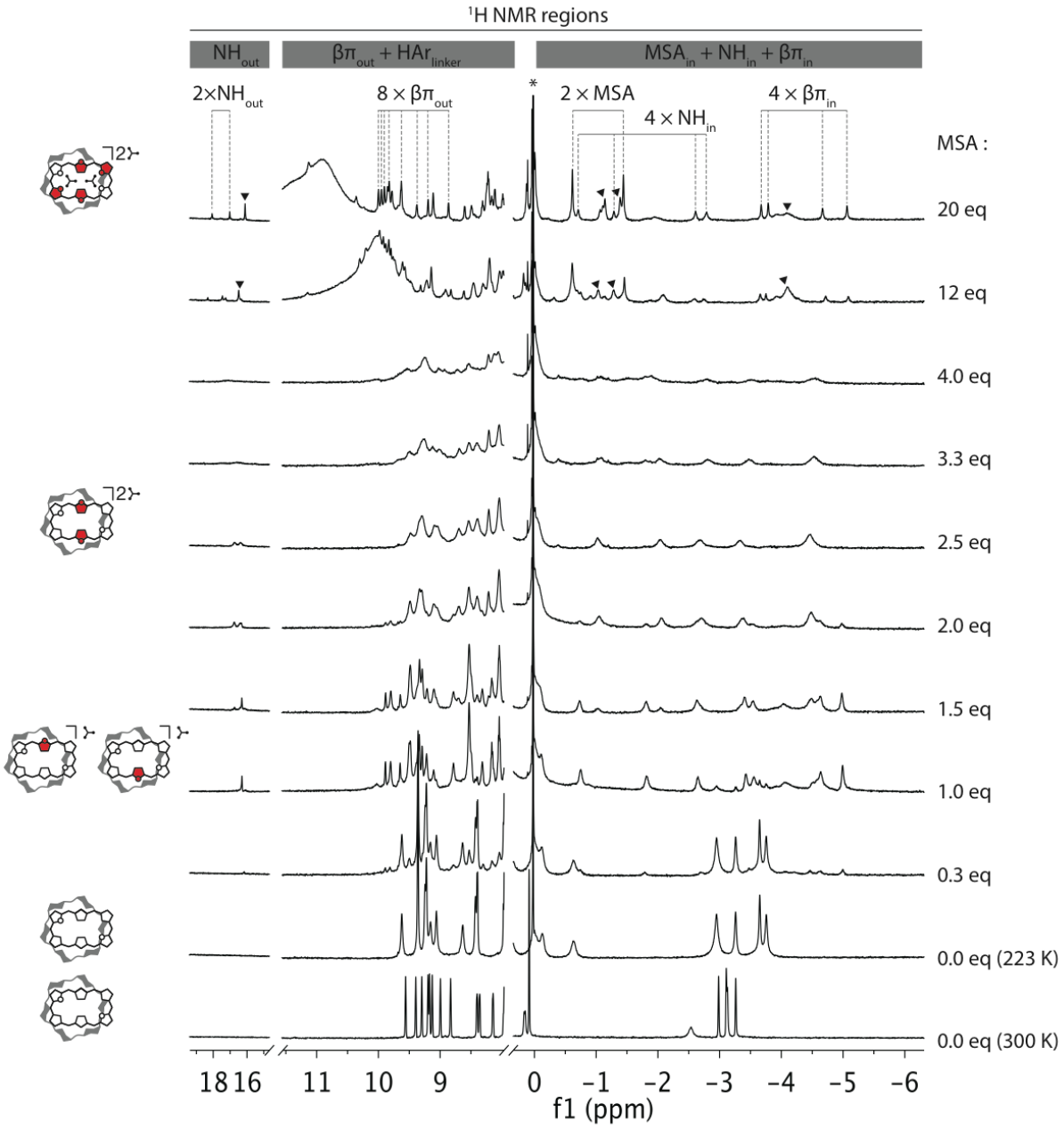

▼: ^{T}**[26]HCD•4H^{+}⊃MSA^{-}** contamination and *: impurities.

3.3. Variable temperature spectra of ^{R}**[26]HCD•4H^{+}⊃2MSA^{-}**, from 223 K to 303 K**,** leading to the thermodynamic ^{T}**[26]HCD•4H^{+}⊃MSA^{-}** (600 MHz, CD_2Cl_2)

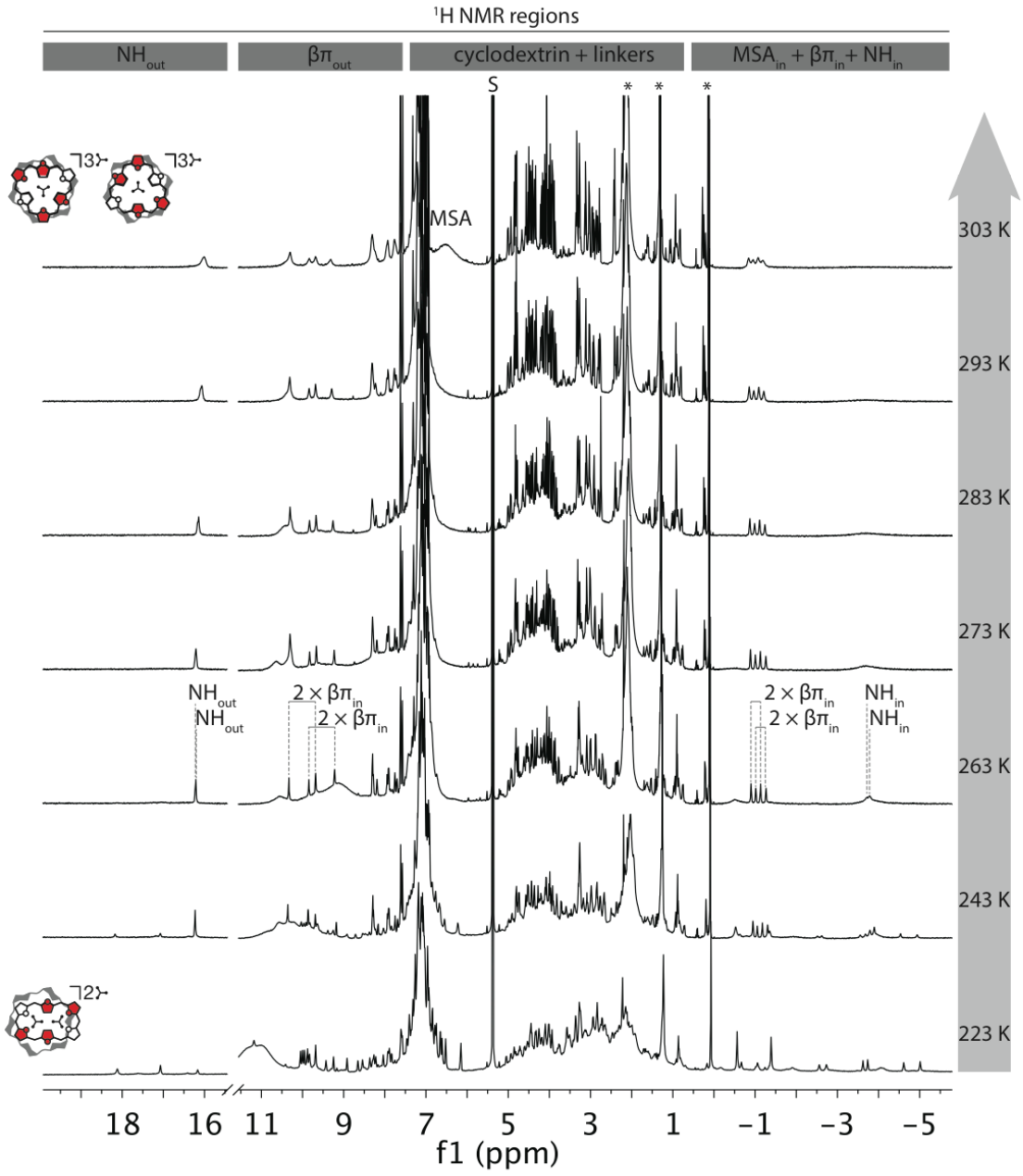

S: solvent and *: impurities.

3.4. VT ^{1}H NMR spectra of ^{T}**[26]HCD•4H^{+}⊃MSA^{-}** (CD_2Cl_2, 600 MHz, from 303 K to 223 K)

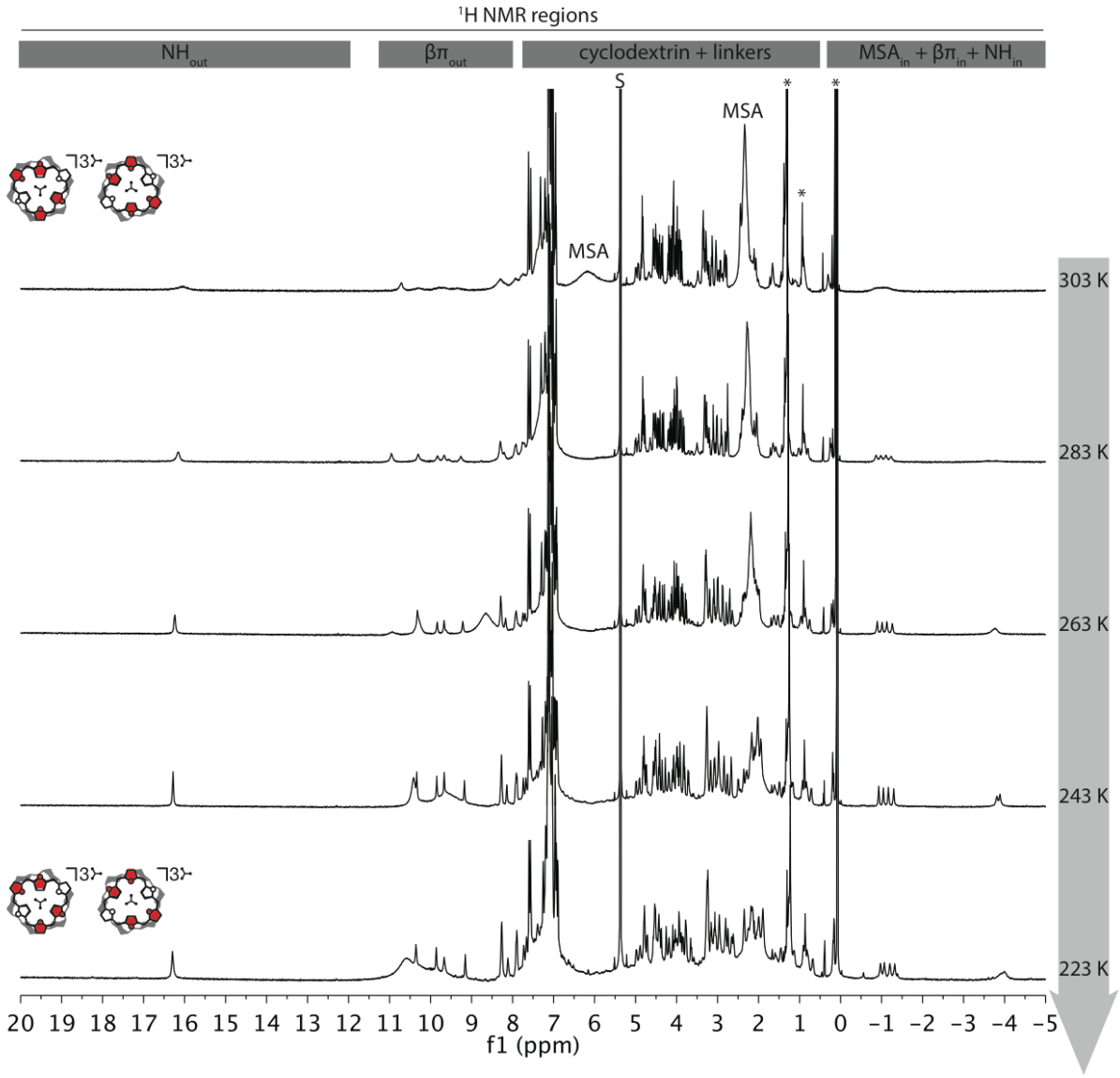

Note: no trace of ^{R}**[26]HCD•4H^{+}⊃2MSA^{-}** (kinetic product) was detected along the VT ^{1}H NMR of ^{T}**[26]HCD•4H^{+}⊃MSA^{-}** (thermodynamic product) from 303 K to 223 K. S: solvent and *: impurities.

3.5. Titration of **[28]HCD** with MSA (600 MHz, CD_2Cl_2, 223 K)

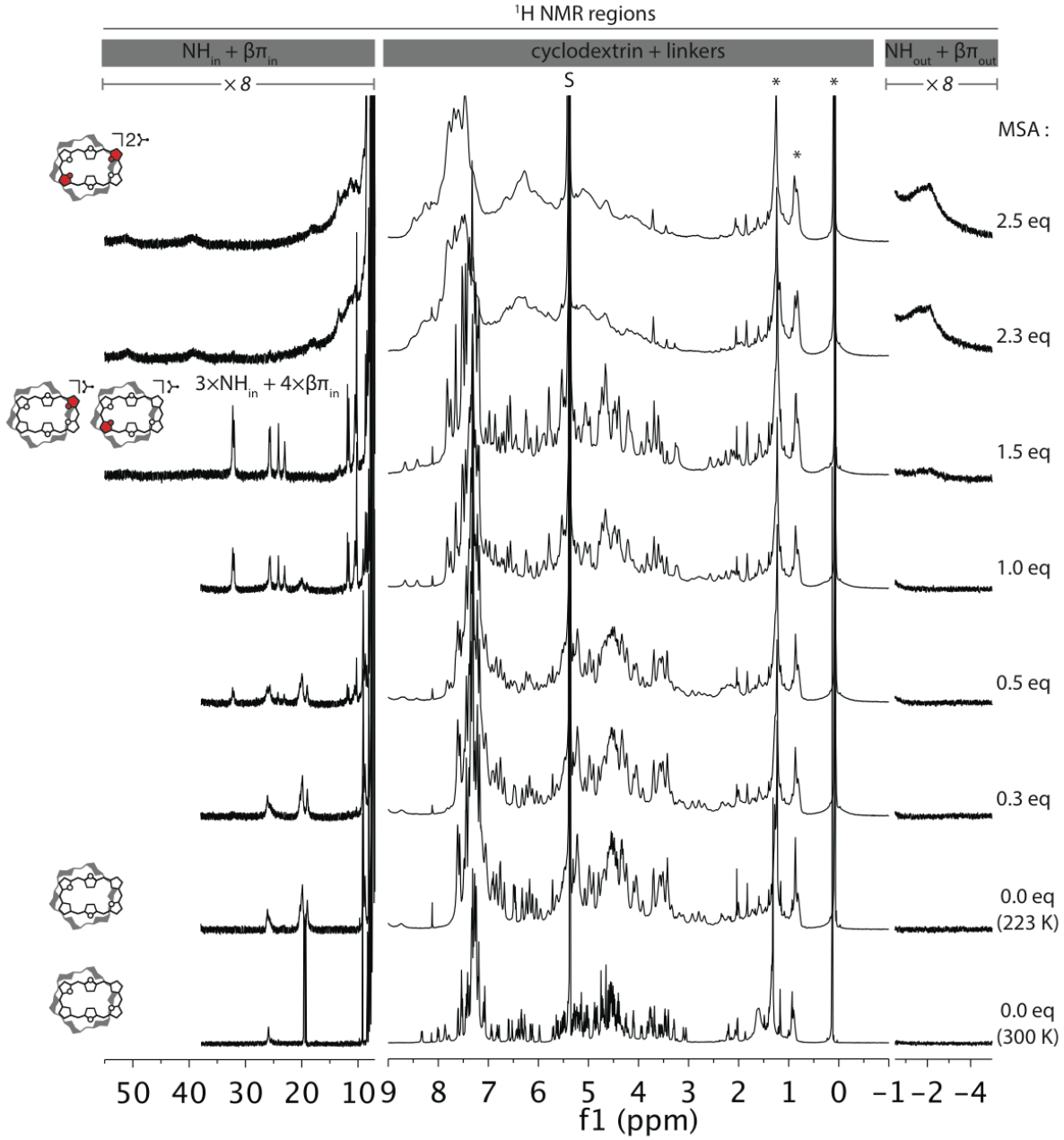

S: solvent and *: impurities.

3.6. Variable temperature spectra of ^{R}**[28]HCD•2H^{+}**, from 223 K to 313 K, leading to the thermodynamic ^{T}**[28]HCD•2H^{+}** (600 MHz, CD_2Cl_2)

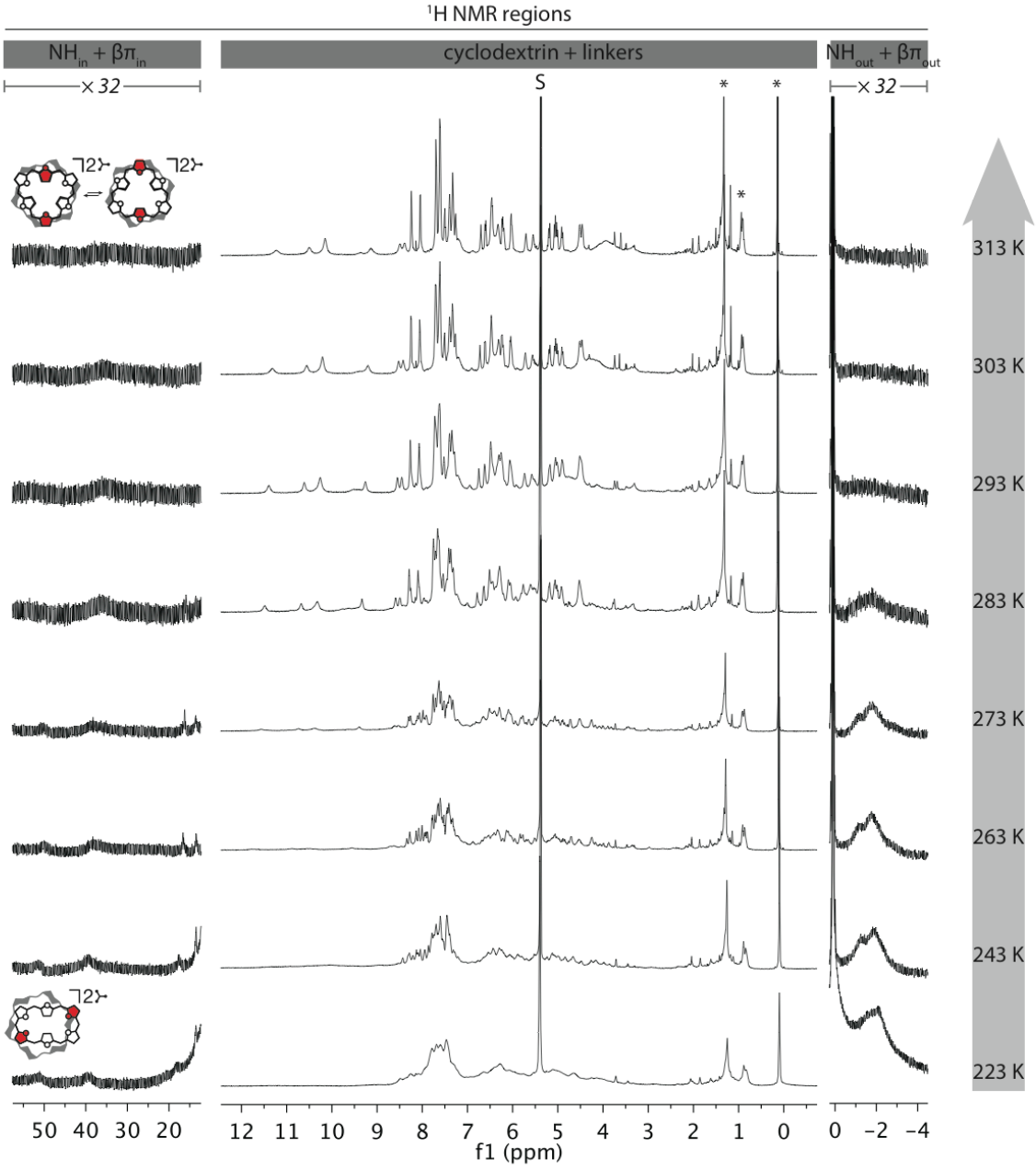

S: solvent and *: impurities.

3.7. VT ^{1}H NMR spectra of ^{T}**[28]HCD•2H^{+}** (600 MHz, CD_2Cl_2, from 313 K to 203 K)

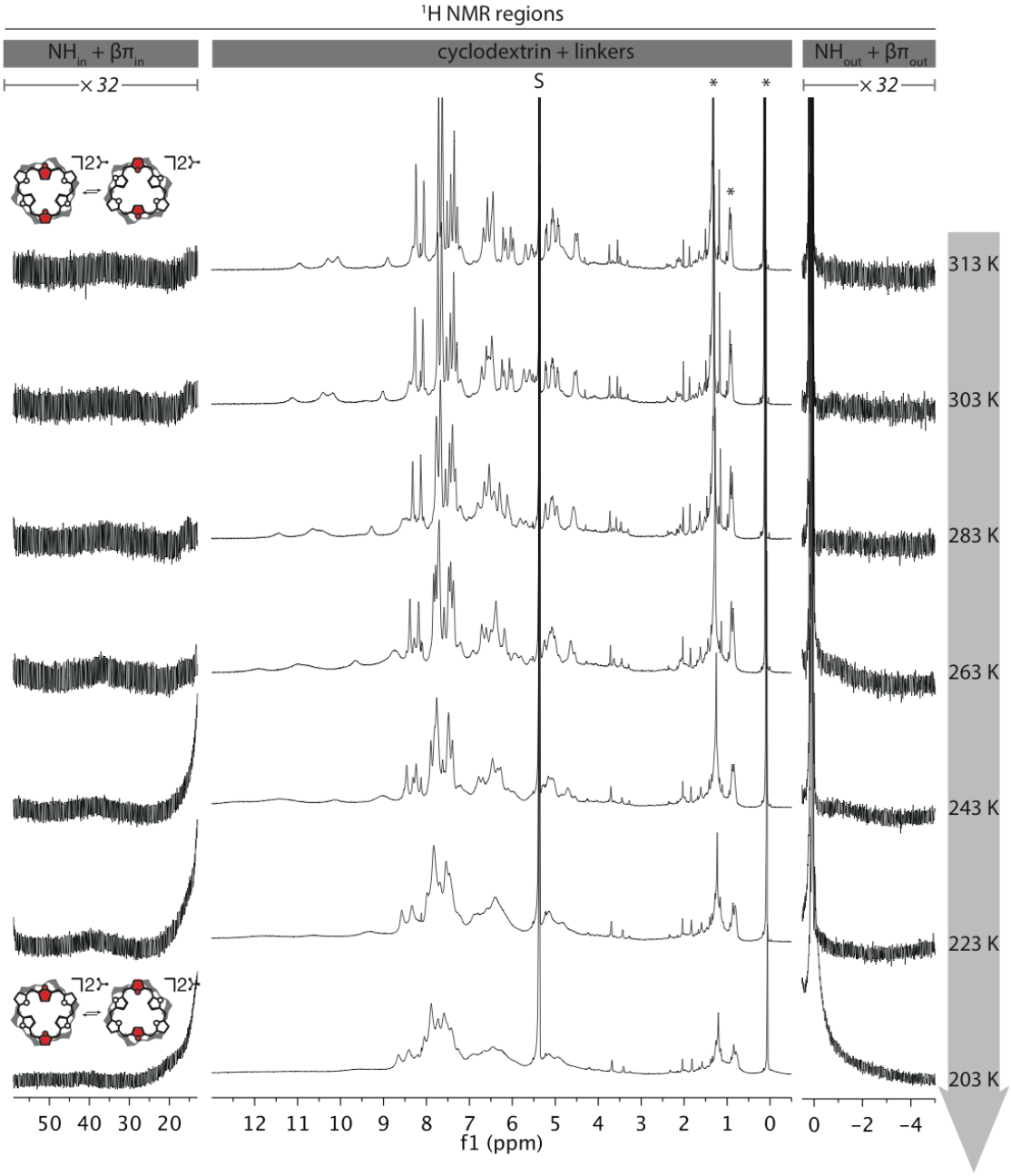

Note: no trace of ^{R}**[28]HCD•2H^{+}** (kinetic product) was detected along the VT ^{1}H NMR of ^{T}**[28]HCD•2H^{+}** (thermodynamic product) from 313 K to 203 K. S: solvent and *: impurities.

4. NMR descriptions

4.1. ^{R}[26]HCD•4H^{+}⊃2MSA^{-} (partial NMR description)

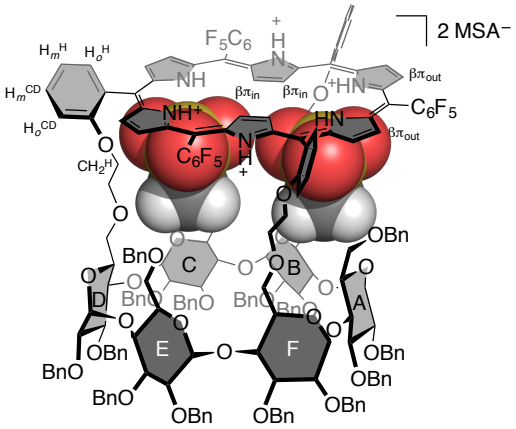

Note : ^{R}[26]HCD•4H^{+}⊃2MSA^{-} was inevitably contaminated by the thermodynamic triangular species.

^{1}H NMR (CD_2Cl_2, 600MHz, 223 K) δ -5.01 (s_b, 1H, $\beta\pi_{in}$), -4.61 (s_b, 1H, $\beta\pi_{in}$), -3.74 (s_b, 1H, $\beta\pi_{in}$), -3.62 (s_b, 1H, $\beta\pi_{in}$), -2.74 (s_b, 1H, NH_{in}), -2.56 (s_b, 1H, NH_{in}), -1.39 (s_b, 3H, $CH_3{}^{MSA}{}_{in}$), -1.06 (s_b, 1H, NH_{in}), -0.67 (s_b, 1H, NH_{in}), -0.56 (s_b, 3H, $CH_3{}^{MSA}{}_{in}$), 1.20-5.17 (m, 84H, 6×H1 + 6×H2 + 6×H3 + 6×H4 + 6×H5 + 6×$CH_2$6 + 15×$CH_2{}^{Bn}$ + 3×$CH_2{}^{CD}$ + 3×$CH_2{}^{H}$), 6.16 (d_b, *J* = 8.2 Hz, 1H, HAr^{Bn}), 6.46-6.70 (m, 75H, 74×HAr^{Bn} + $H_o{}^{CD}$), 7.83 (d_b, *J* = 8.8 Hz, 1H, $H_o{}^{CD}$), 7.86-7.95 (m, 2H, $H_o{}^{CD}$ + $H_m{}^{H}$), 8.04 (t_b, *J* = 7.6 Hz, 1H, $H_m{}^{H}$), 8.22 (t_b, *J* = 7.0 Hz, 1H, $H_m{}^{CD}$), 8.26 (t_b, *J* = 8.0 Hz, 1H, $H_m{}^{H}$), 8.36 (t_b, *J* = 8.5 Hz, 1H, $H_m{}^{CD}$), 8.54 (t_b, *J* = 8.3 Hz, 1H, $H_m{}^{CD}$), 8.65 (s_b, 1H, $H_o{}^{H}$), 8.92 (s_b, 1H, $\beta\pi_{out}$), 9.25 (s_b, 1H, $\beta\pi_{out}$), 9.43 (s_b, 1H, $\beta\pi_{out}$), 9.65-9.71 (m, 2H, $\beta\pi_{out}$ + $H_o{}^{H}$), 9.83 (d_b, *J* = 7.0 Hz, 1H, $H_o{}^{H}$), 9.88 (s_b, 1H, $\beta\pi_{out}$), 9.95 (s_b, 1H, $\beta\pi_{out}$), 10.00 (s_b, 1H, $\beta\pi_{out}$), 10.05 (s_b, 1H, $\beta\pi_{out}$), 17.07 (s_b, 1H, NH_{out}), 18.12 (s_b, 1H, NH_{out}).

Partial ^{13}C from 2D HSQC (CD_2Cl_2, 600 MHz, 223 K) δ 34.3 ($CH_3{}^{MSA}{}_{in}$), 37.1 ($CH_3{}^{MSA}{}_{in}$), 60.0-85.0 (6×C2, 6×C3, 6×C4, 6×C5, 6×C6, 3×$CH_2{}^{CD}$, 3×$CH_2{}^{H}$, 15×$CH_2{}^{Bn}$), 93.7 (C1), 97.2 (C1), 99.5 (C1), 99.7 (C1), 101.2 (C1), 103.1 (C1), 111.0 ($C_o{}^{CD}$), 112.2 ($C_o{}^{CD}$), 113.4 ($C_o{}^{CD}$), 120.7 ($C_m{}^{H}$), 121.0 ($C_m{}^{H}$), 121.9 ($C_m{}^{H}$), 121.9 (*C*-$\beta\pi_{in}$), 122.1 (*C*-$\beta\pi_{in}$), 124.0-130.0 (75×CH^{Ar}), 130.8 (*C*-$\beta\pi_{out}$), 130.9 (*C*-$\beta\pi_{out}$), 132.7 (*C*-$\beta\pi_{out}$), 133.0 (*C*-$\beta\pi_{out}$), 134.2 (*C*-$\beta\pi_{out}$), 134.3 ($C_m{}^{CD}$), 134.5 (*C*-$\beta\pi_{out}$), 134.8 (*C*-$\beta\pi_{out}$), 136.0 (*C*-$\beta\pi_{out}$), 136.1 ($C_o{}^{H}$ + $C_m{}^{CD}$), 137.0 ($C_o{}^{H}$), 137.1 ($C_o{}^{H}$), 137.2 ($C_m{}^{CD}$).

4.2. ^{T}**[26]HCD•4H^{+}⊃MSA^{-}** (1:1 mixture of S_p,*P* and R_p,*M* diastereomers)

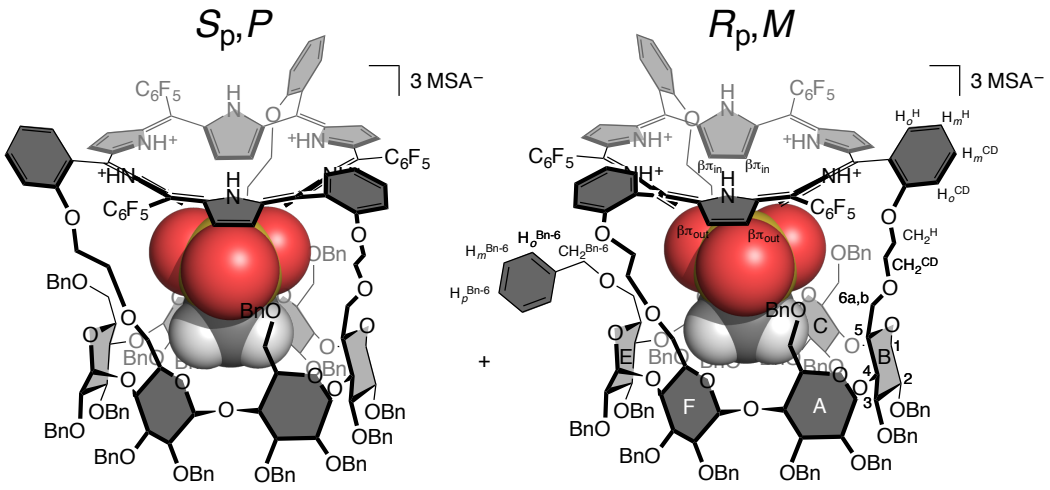

Note: absolute assignment of the two NMR patterns to either S_p,*P* or R_p,*M* diastereomer was not possible. These patterns have been therefore labeled "α" and "β".

^{19}F NMR (CD_2Cl_2, 565 MHz, 263 K) δ -161.61 (br, 3F, 3×F_m), -161.14 (br, 3F, 3×F_m), -157.93 (br, 3F, 3×F_m), -157.47 (br, 3F, 3×F_m), -144.01 (br, 3F, 3×F_p), -143.67 (br, 3F, 3×F_p), -140.11 (br, 3F, 3×F_o), -139.72 (br, 3F, 3×F_o), -139.22 (br, 3F, 3×F_o), -139.06 (br, 3F, 3×F_o).

^{1}H NMR (CD_2Cl_2, 600 MHz, 263 K) δ -3.85 (s_b, 3H, 3×NH_{in}^{β}), -3.76 (s_b, 3H, 3×NH_{in}^{α}), -1.28 (s_b, 3H, 3×$\beta\pi_{in}^{\alpha}$), -1.16 (s_b, 3H, 3×$\beta\pi_{in}^{\beta}$), -1.03 (s_b, 3H, 3×$\beta\pi_{in}^{\alpha}$), -0.92 (s_b, 3H, 3×$\beta\pi_{in}^{\beta}$), 0.20 (s_b, 3H, $CH_3^{MSA}{}_{in}^{\alpha}$), 0.22 ($s_b$, 3H, $CH_3^{MSA}{}_{in}^{\beta}$), 0.75 ($d_b$, *J*= 12.5 Hz, 3H, H6a$^{A,C,E-\beta}$), 0.97 ($d_b$, *J*= 12.9 Hz, 3H, H6a$^{A,C,E-\alpha}$), 1.20 ($d_b$, *J*= 14.3 Hz, 3H, H6a$^{B,D,F-\beta}$), 1.53 ($d_b$, *J*= 11.7 Hz, 3H, H6a$^{B,D,F-\alpha}$), 1.96-2.01 (m, 6H, H6b$^{A,C,E-\alpha}$ + H6b$^{A,C,E-\beta}$), 2.07 (br, 3H, H6b$^{B,D,F-\alpha}$), 2.11-2.26 (m, 12H, C*H*H^{Bn}-6$^{A,C,E-\beta}$ + H5$^{A,C,E-\alpha}$ + H5$^{B,D,F-\alpha}$ + H5$^{A,C,E-\beta}$), 2.34 (d_b, *J*= 14.6 Hz, 3H, H6b$^{B,D,F-\beta}$), 2.38 (d_b, *J*= 9.2 Hz, 3H, H5$^{B,D,F-\beta}$), 2.62 (d_b, *J*= 10.9 Hz, 3H, C*H*H^{Bn}-6$^{A,C,E-\alpha}$), 2.66-2.74 (m, 6H, CH*H*^{Bn}-6$^{A,C,E-\alpha}$ + H2$^{A,C,E-\alpha}$), 2.78 (dd_b, $^{3}J_{1,2}$ = 2.1 Hz, $^{3}J_{2,3}$ = 9.2 Hz, 3H, H2$^{B,D,F-\alpha}$), 2.83-2.90 (m, 6H, CH*H*^{Bn}-6$^{A,C,E-\beta}$ + H2$^{A,C,E-\beta}$), 2.94-3.05 (m, 6H, C*H*H$^{H\text{-}B,D,F-\alpha}$ + H2$^{B,D,F-\beta}$), 3.06-3.12 (m, 6H, H4$^{A,C,E-\alpha}$ + H4$^{A,C,E-\beta}$), 3.20 (t_b, *J*= 9.8 Hz, 3H, C*H*H$^{H\text{-}B,D,F-\beta}$), 3.23-3.34 (m, 18H, H3$^{A,C,E-\alpha}$ + H3$^{A,C,E-\beta}$ + H3$^{B,D,F-\alpha}$ + H3$^{B,D,F-\beta}$ + H4$^{B,D,F-\alpha}$ + H4$^{B,D,F-\beta}$), 3.77 (d, ^{2}J= 12.1 Hz, 3H, 3×H^{Bn}), 3.85 (d, ^{2}J= 11.8 Hz, 3H, 3×H^{Bn}), 3.87 (d, ^{2}J= 12.7 Hz, 3H, 3×H^{Bn}), 3.93-4.08 (m, 18H, H1$^{B,D,F-\alpha}$ + CH*H*$^{H\text{-}B,D,F-\alpha}$ + 12×H^{Bn}), 4.13 (d, ^{2}J= 12.9 Hz, 3H, 3×H^{Bn}), 4.20 (d_b, *J*= 10.1 Hz, 3H, CH*H*$^{H\text{-}B,D,F-\beta}$), 4.29 (d_b, $^{3}J_{1,2}$= 3.3 Hz, 3H, H1$^{A,C,E-\beta}$), 4.35 (d_b, $^{3}J_{1,2}$= 3.1 Hz, 3H, H1$^{A,C,E-\alpha}$), 4.39-4.46 (m, 6H, H1$^{B,D,F-\beta}$ + 3×H^{Bn}), 4.48-4.59 (m, 12H, C*H*H$^{CD\text{-}B,D,F-\beta}$ + 9×H^{Bn}), 4.62 (t_b, *J*= 10.2 Hz, 3H, C*H*H$^{CD\text{-}B,D,F-\alpha}$), 4.76 (d, ^{2}J= 12.3 Hz, 3H, 3×H^{Bn}), 4.78-4.85 (m, 9H, 9×H^{Bn}), 4.92 (d_b, *J*= 10.4 Hz, 3H, CH*H*$^{CD\text{-}B,D,F-\beta}$), 4.99 (d_b, *J*= 10.7 Hz, 3H, CH*H*$^{CD\text{-}B,D,F-\alpha}$), 6.90-7.23 (m, 120H, 120×HAr^{Bn}), 7.21 (br, 6H, 2×H_o^{Bn}-6$^{A,C,E-\alpha}$), 7.29 (br, 6H, 2×H_o^{Bn}-6$^{A,C,E-\beta}$), 7.55-7.59 (m, 9H, 2×H_m^{Bn}-6$^{A,C,E-\alpha}$ + H_p^{Bn}-6$^{A,C,E-\alpha}$), 7.59-7.63 (m, 9H, 2×H_m^{Bn}-6$^{A,C,E-\beta}$ + H_p^{Bn}-6$^{A,C,E-\beta}$), 7.70 (br, 3H, $H_m$$^{H\text{-}B,D,F-\alpha}$), 7.75 (br, 3H, $H_m$$^{H\text{-}B,D,F-\beta}$), 7.86-7.97 (m, 6H, $H_o$$^{CD\text{-}B,D,F-\beta}$ + $H_o$$^{CD\text{-}B,D,F-\alpha}$), 8.18 ($s_b$, 3H, $H_o$$^{H\text{-}B,D,F-\alpha}$), 8.23-8.35 (m, 9H, $H_o$$^{CD\text{-}B,D,F-\beta}$ + $H_m$$^{H\text{-}B,D,F-\alpha}$ + $H_m$$^{CD\text{-}B,D,F-\beta}$), 9.21 ($s_b$, 3H, 3×$\beta\pi_{out}^{\alpha}$), 9.69 ($s_b$, 3H, 3×$\beta\pi_{out}^{\beta}$), 9.85 ($s_b$, 3H, 3×$\beta\pi_{out}^{\alpha}$), 10.34 ($s_b$, 3H, 3×$\beta\pi_{out}^{\beta}$), 16.14 ($s_b$, 3H, 3×$NH_{out}^{\beta}$) 16.16 ($s_b$, 3H, 3×$NH_{out}^{\alpha}$).

^{13}C from 2D HSQC (CD_2Cl_2, 600 MHz, 263 K) δ 38.3 ($CH_3^{MSA_{in}\alpha}$ + $CH_3^{MSA_{in}\beta}$), 68.1 ($CH_2^{CD\text{-}B,D,F\text{-}\beta}$), 69.2 ($CH_2^{CD\text{-}B,D,F\text{-}\alpha}$), 69.3 ($CH_2$-$6^{A,C,E\text{-}\alpha}$), 69.4-69.8 (3×C5, CH_2-$6^{B,D,F\text{-}\alpha}$, CH_2-$6^{A,C,E\text{-}\beta}$), 70.2 (CH_2-$6^{B,D,F\text{-}\beta}$), 70.5 (3×C5), 70.6 (3×CH_2^{Bn}), 71.1 (3×C5 + $CH_2^{H\text{-}B,D,F\text{-}\alpha}$), 71.2-71.7 (9×$CH_2^{Bn}$), 72.1 ($CH_2^{Bn}$-$6^{A,C,E\text{-}\beta}$), 72.2 ($CH_2^{Bn}$-$6^{A,C,E\text{-}\alpha}$), 72.5 ($C5^{B,D,F\text{-}\beta}$), 73.3 ($CH_2^{H\text{-}B,D,F\text{-}\beta}$), 75.1-75.8 (12×$CH_2^{Bn}$), 76.5 ($C2^{A,C,E\text{-}\alpha}$), 77.5 ($C2^{A,C,E\text{-}\beta}$), 77.9 ($C2^{B,D,F\text{-}\alpha}$), 78.0 ($C2^{B,D,F\text{-}\beta}$), 79.1 ($C3^{A,C,E\text{-}\alpha}$ + $C3^{B,D,F\text{-}\alpha}$ + $C3^{A,C,E\text{-}\beta}$ + $C3^{B,D,F\text{-}\beta}$), 81.0-81.2 ($C4^{A,C,E\text{-}\alpha}$ + $C4^{B,D,F\text{-}\alpha}$ + $C4^{A,C,E\text{-}\beta}$ + $C4^{B,D,F\text{-}\beta}$), 99.2 ($C1^{B,D,F\text{-}\beta}$), 100.0 ($C1^{B,D,F\text{-}\alpha}$), 100.9 ($C1^{A,C,E\text{-}\beta}$), 101.0 ($C1^{A,C,E\text{-}\alpha}$), 111.7 ($C_o^{CD\text{-}B,D,F\text{-}\beta}$), 111.8 ($C_o^{CD\text{-}B,D,F\text{-}\beta}$), 121.3 ($C_m^{H\text{-}B,D,F\text{-}\beta}$), 121.4 ($C_m^{H\text{-}B,D,F\text{-}\alpha}$), 126.0-129.0 (150×$CH^{Ar\text{-}Bn}$), 131.7 (3×*C*-$\beta\pi_{in}^{\alpha}$), 132.0 (3×*C*-$\beta\pi_{in}^{\beta}$), 132.3 (3×*C*-$\beta\pi_{in}^{\alpha}$), 132.8 (3×*C*-$\beta\pi_{in}^{\beta}$), 132.8 (3×*C*-$\beta\pi_{out}^{\beta}$), 132.9 (3×*C*-$\beta\pi_{out}^{\alpha}$), 134.7 (3×*C*-$\beta\pi_{out}^{\alpha}$), 136.1 (3×*C*-$\beta\pi_{out}^{\beta}$), 138.2 ($C_m^{CD\text{-}B,D,F\text{-}\alpha}$ + $C_m^{CD\text{-}B,D,F\text{-}\beta}$), 140.8 ($C_o^{H\text{-}B,D,F\text{-}\alpha}$), 141.0 ($C_o^{H\text{-}B,D,F\text{-}\beta}$).

4.3. ^{1}H NMR assignment of **^{T}[26]HCD•4H^{+}⊃MSA^{-}** (600 MHz, CD_2Cl_2, 263 K)

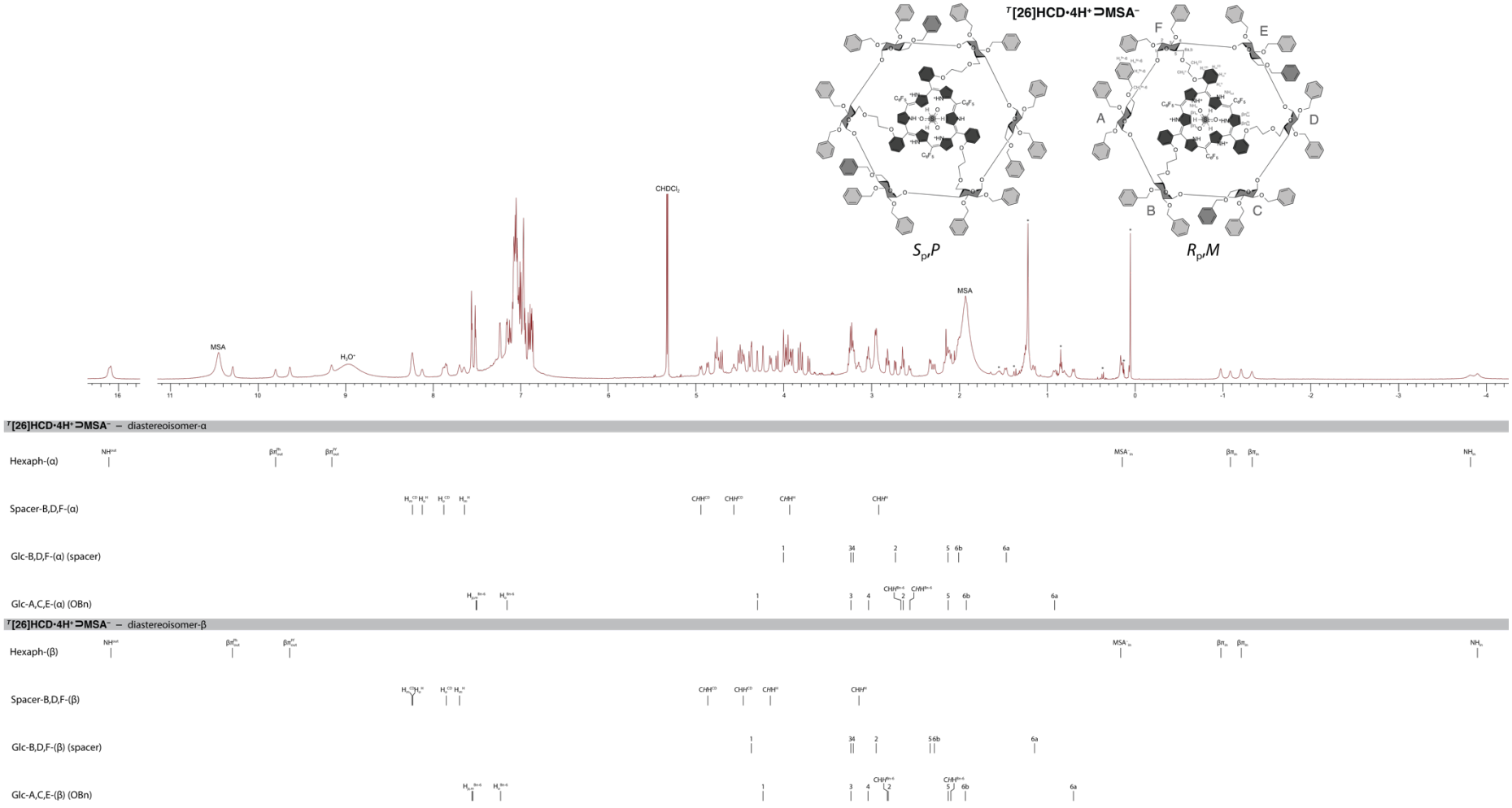

4.4. ^{T}**[28]HCD•2H^{+}** (average spectrum of diastereomers)

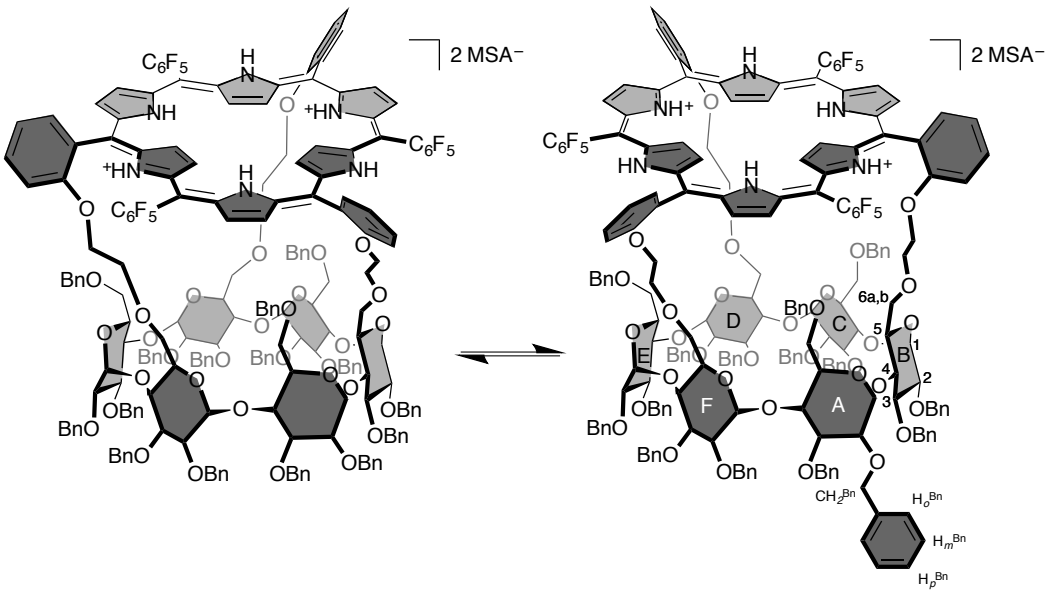

Note: average spectrum showing only the cyclodextrin part (the hexaphyrin cap is coalescing, see the article). The coalescence of the hexaphyrin cap and the primary rim ($CH_2$6-OBn and CH_2-linker) prevent the absolute determination of the glucose units. Thus, the two sets of signals corresponding to the two glucose units (*i.e.* A,C,E and B,D,F) of the C_3 symmetrical averaged ^{T}**[28]HCD•2H^{+}** have been labeled " Glc " and " Glc' ".

^{1}H NMR (CD_2Cl_2, 600 MHz, 313 K) δ 4.34-4.53 (m, 6H, 3×H2^{Glc} + 3×H2$^{Glc'}$), 4.86 (d_b, *J* = 14.6 Hz, 3H, 3×C*H*H^{Bn}-2^{Glc}), 4.97 (d_b, *J* = 14.2 Hz, 3H, 3×C*H*H^{Bn}-2$^{Glc'}$), 5.02 (d_b, *J* = 14.4 Hz, 3H, 3×CH*H*^{Bn}-2^{Glc}), 5.14 (d_b, *J* = 14.1 Hz, 3H, 3×CH*H*^{Bn}-2$^{Glc'}$), 5.50 (br, 3H, 3×H4^{Glc}), 5.66 (br, 3H, 3×H4$^{Glc'}$), 5.92-6.03 (m, 6H, 3×H3^{Glc} + 3×C*H*H^{Bn}-3$^{Glc'}$), 6.16-6.21 (m, 6H, 3×H3$^{Glc'}$ + 3×C*H*H^{Bn}-3^{Glc}), 6.37-6.49 (m, 6H, 3×H1$^{Glc'}$ + 3×CH*H*^{Bn}-3$^{Glc'}$), 6.56 (d_b, *J* = 9.7 Hz, 3H, 3×CH*H*^{Bn}-3^{Glc}), 6.66 (s_b, 3H, 3×H1^{Glc}), 7.21 (br, 3H, 3×H$_p$^{Bn}-2$^{Glc'}$), 7.24-7.32 (m, 9H, 6×H$_m$^{Bn}-2$^{Glc'}$ + 3×H$_p$^{Bn}-2^{Glc}), 7.35 (br, 6H, 6×H$_m$^{Bn}-2^{Glc}), 7.45 (t_b, *J* = 7.4 Hz, 3H, 3×H$_p$^{Bn}-3$^{Glc'}$), 7.51-7.61 (m, 15H, 6×H$_m$^{Bn}-3$^{Glc'}$ + 3×H$_p$^{Bn}-3^{Glc} + 6×H$_o$^{Bn}-2^{Glc}), 7.61-7.71 (m, 12H, 6×H$_m$^{Bn}-3^{Glc} + 6×H$_o$^{Bn}-2$^{Glc'}$), 8.00 (d_b, *J* = 7.2 Hz, 6H, 6×H$_o$^{Bn}-3$^{Glc'}$), 8.19 (d_b, *J* = 6.8 Hz, 6H, 6×H$_o$^{Bn}-3^{Glc}), 8.34 (br, 3H, 3×H5^{Glc}), 8.45 (br, 3H, 3×H5$^{Glc'}$).

Partial ^{13}C from 2D HSQC (CD_2Cl_2, 600 MHz, 313 K) δ 72.5 (*C*H$_2$^{Bn}-2^{Glc}), 73.2 (*C*H$_2$^{Bn}-2$^{Glc'}$), 75.5 (C5$^{Glc'}$), 77.0 (*C*H$_2$^{Bn}-3$^{Glc'}$), 77.8 (*C*H$_2$^{Bn}-3^{Glc}), 78.3 (C5^{Glc}), 80.2 (C2$^{Glc'}$), 81.3 (C2^{Glc}), 82.5 (C3^{Glc}), 82.6 (C3$^{Glc'}$), 85.0 (C4^{Glc}), 85.3 (C4$^{Glc'}$), 102.7 (C1^{Glc}), 104.4 (C1$^{Glc'}$), 127.3 (C$_p$^{Bn}-3$^{Glc'}$), 127.5 (C$_p$^{Bn}-3^{Glc}), 127.8 (C$_p$^{Bn}-2$^{Glc'}$), 127.9 (C$_p$^{Bn}-2^{Glc}), 128.0 (C$_o$^{Bn}-3$^{Glc'}$), 128.5-129.5 (C$_m$^{Bn}-2$^{Glc'}$, C$_m$^{Bn}-2^{Glc}, C$_m$^{Bn}-3$^{Glc'}$, C$_m$^{Bn}-3^{Glc}, C$_o$^{Bn}-2$^{Glc'}$, C$_o$^{Bn}-2^{Glc}, C$_o$^{Bn}-3^{Glc}).

4.5. ^{1}H NMR assignment of ^{T}**[28]HCD•2H^{+}** (600 MHz, CD_2Cl_2, 313 K)

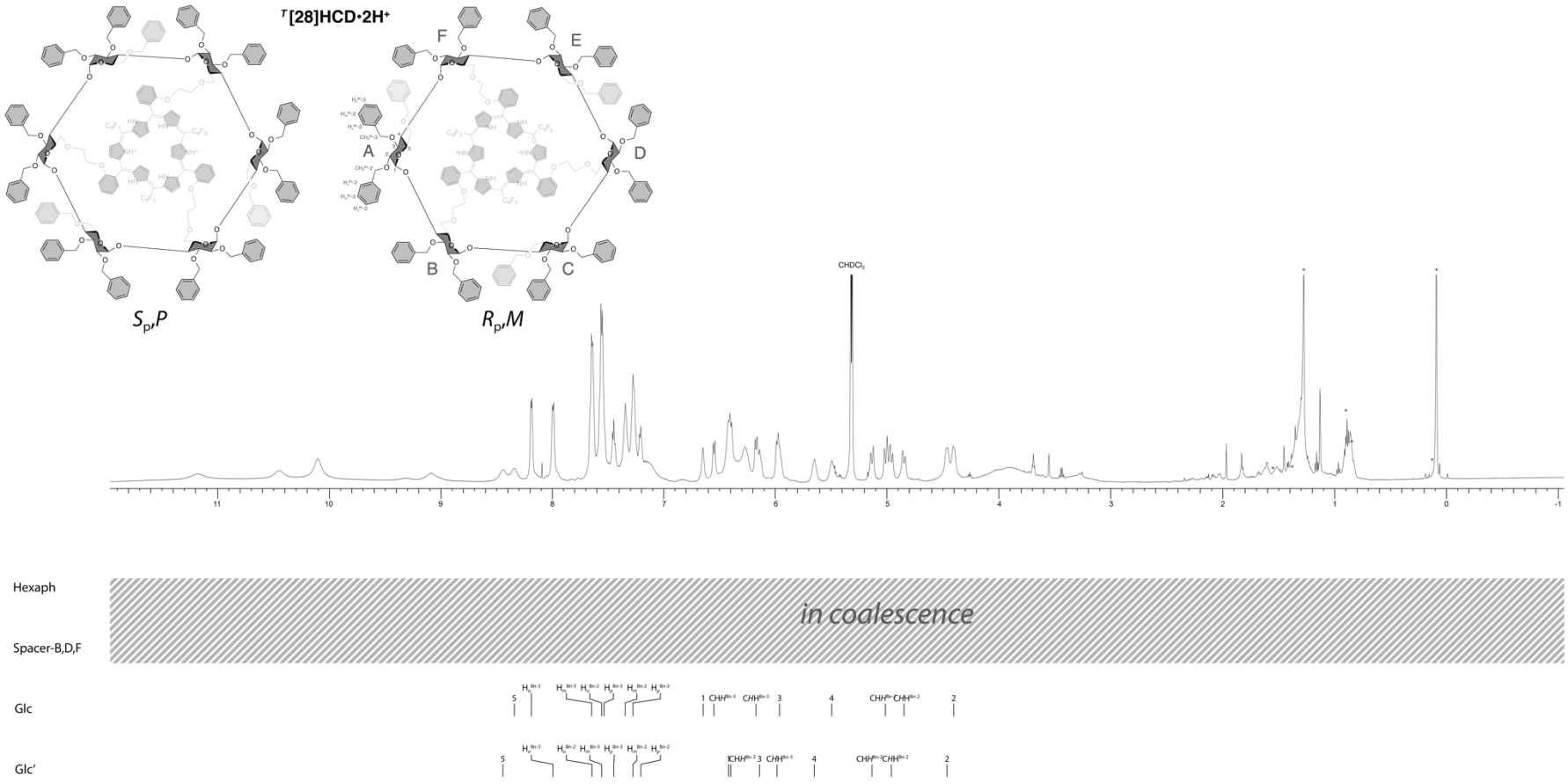

5. NMR spectra of ^{R}[26]HCD•4H^{+}⊃2MSA^{-}

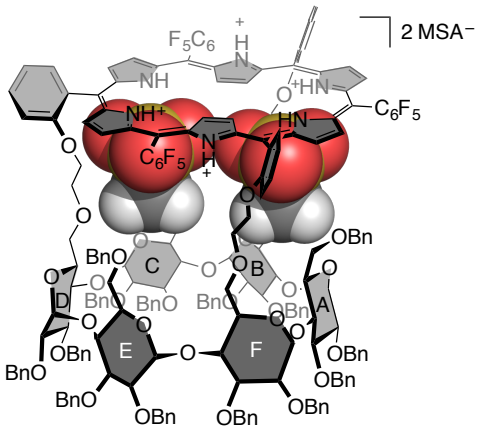

5.1. ^{1}H NMR (600 MHz, CD_2Cl_2, 223 K)

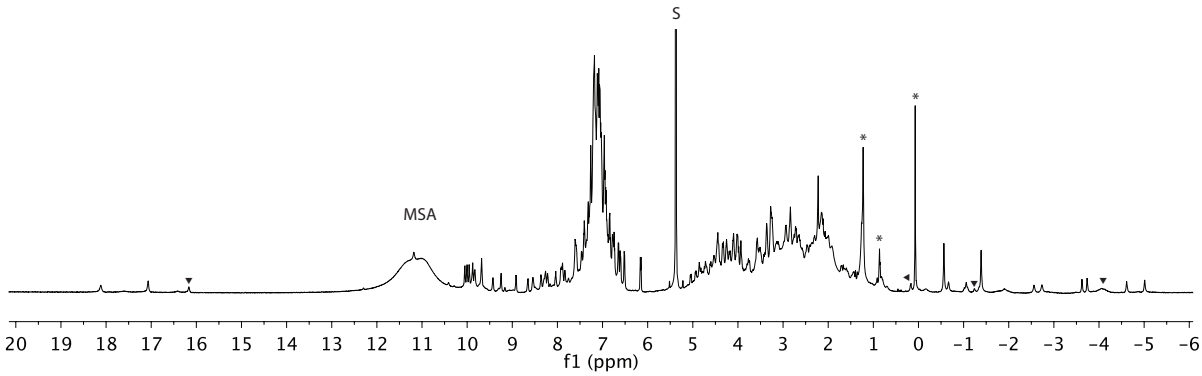

S: solvent, ▼: ^{T}[26]HCD•4H^{+}⊃MSA^{-} contamination and *: impurities.

5.2. 2D COSY (600 MHz, CD_2Cl_2, 223 K)

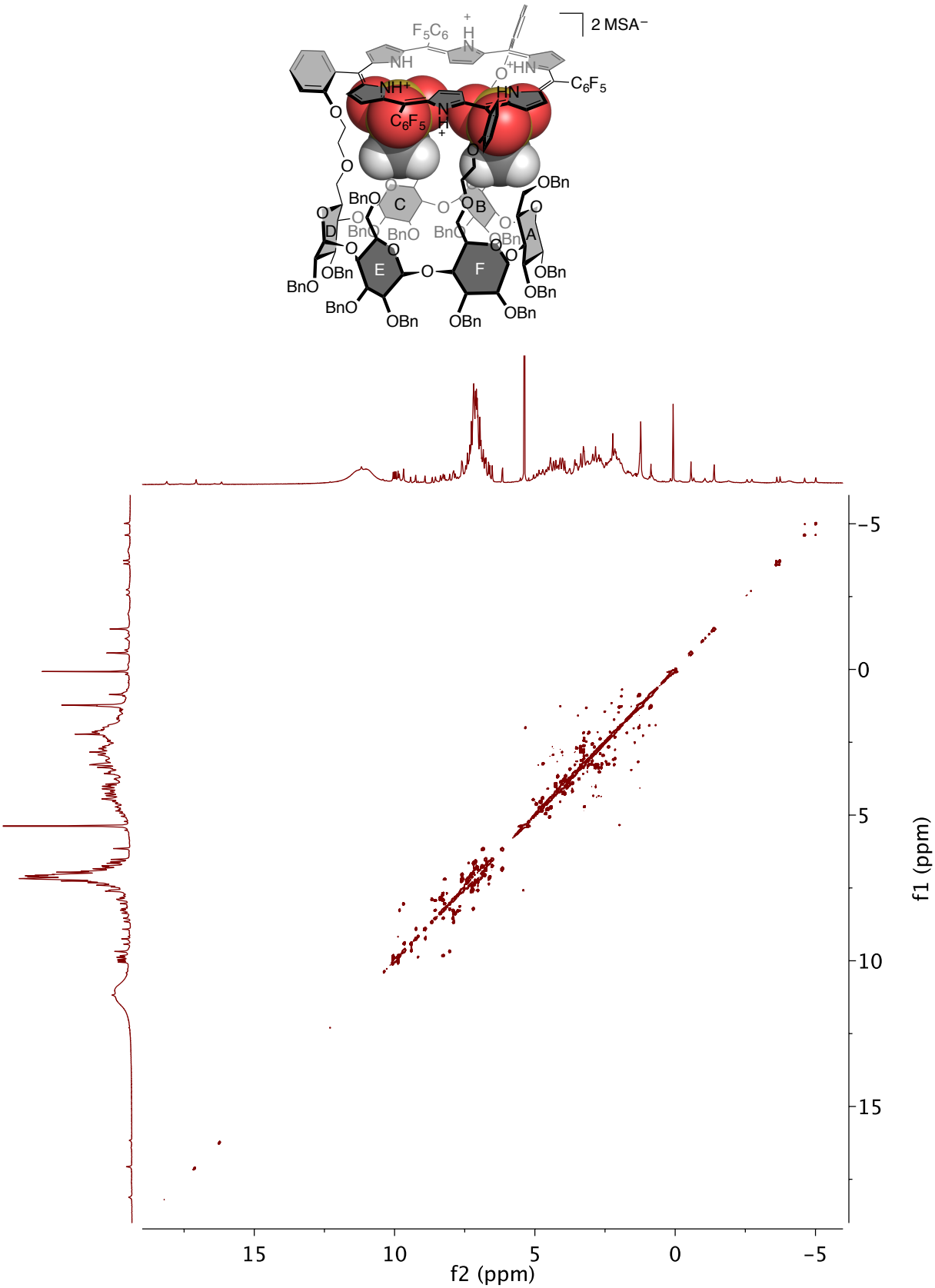

5.3. 2D HSQC-edited (600 MHz, CD_2Cl_2, 223 K)

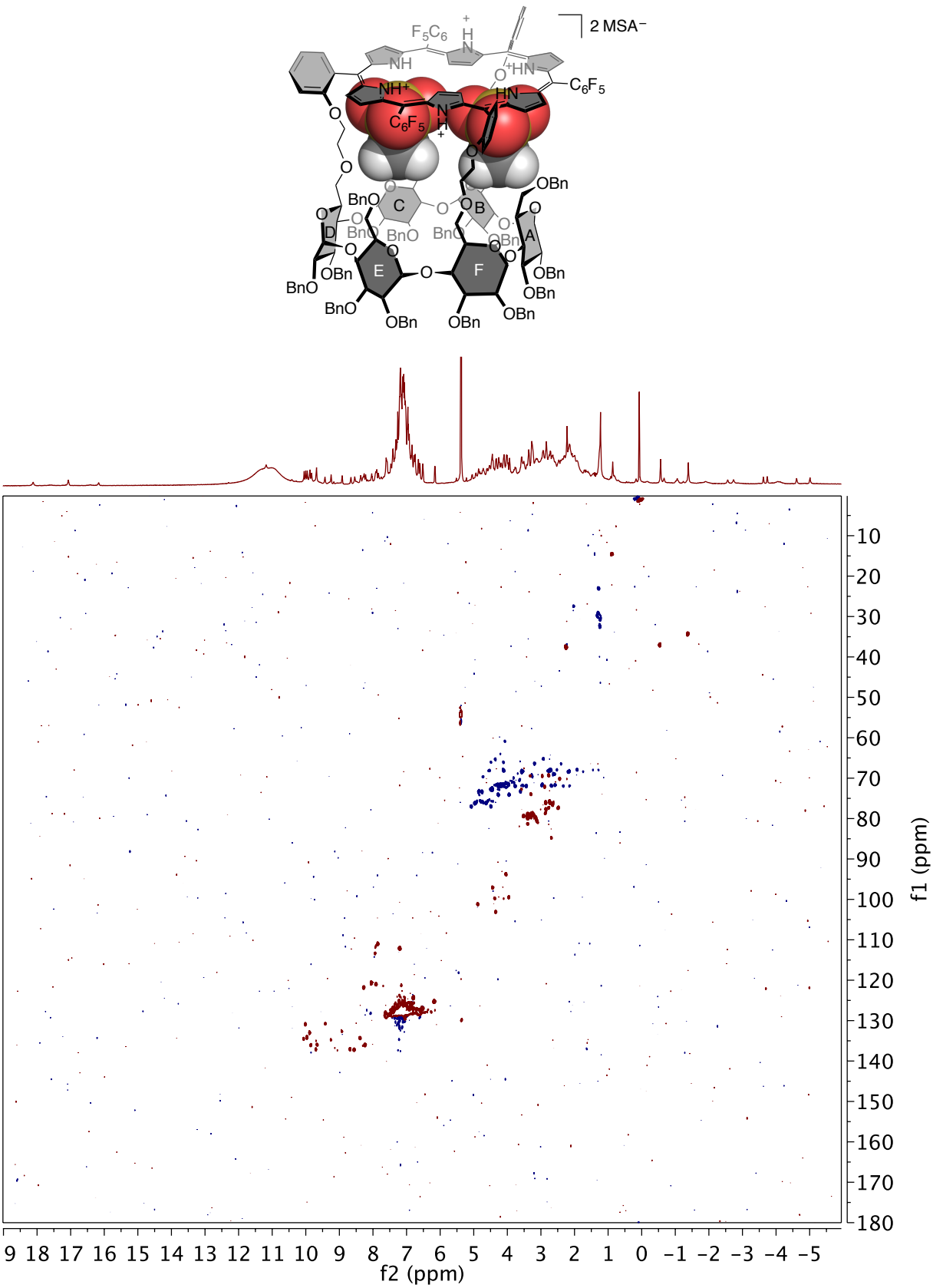

5.4. 2D NOESY (600 MHz, CD_2Cl_2, 223 K, τ = 800 ms)

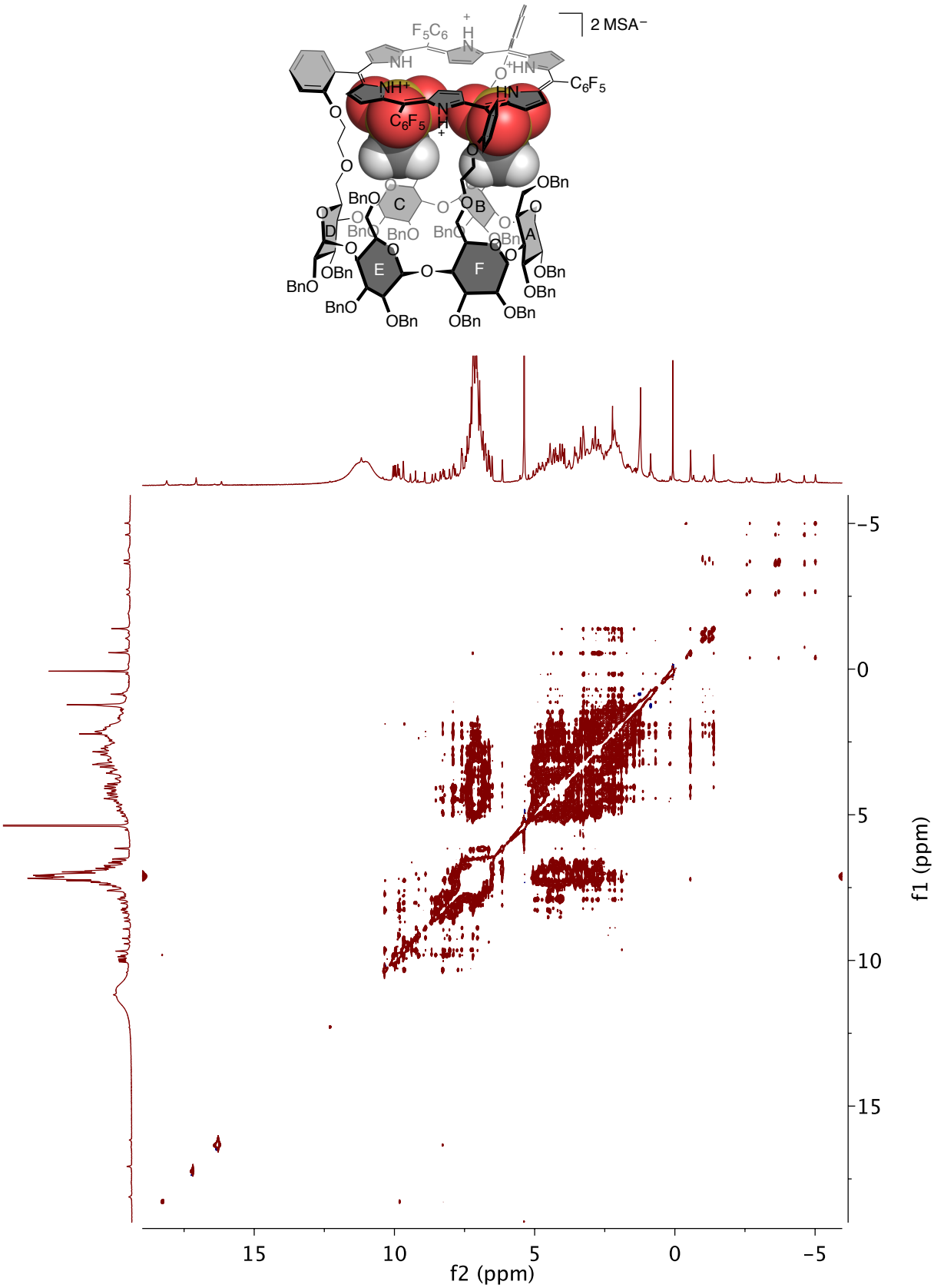

5.5. Zoom on the MSA_{in} correlations region of the 2D NOESY NMR spectrum of ^{R}**[26]HCD•4H^{+}⊃2MSA^{-}** (600 MHz, CD_2Cl_2, 223 K)

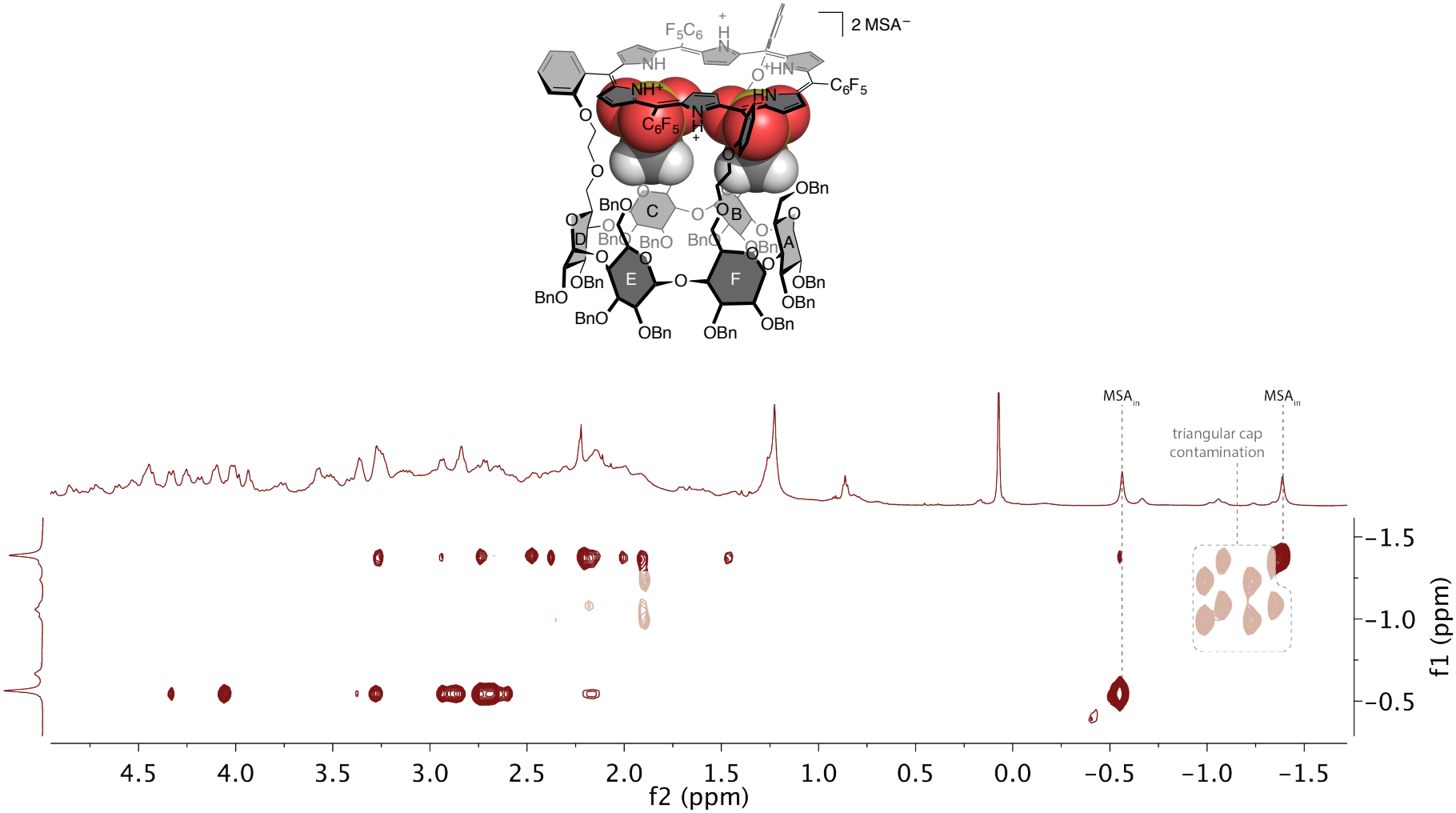

6. NMR spectra of ^{T}[26]HCD•4H^{+}⊃MSA^{-}

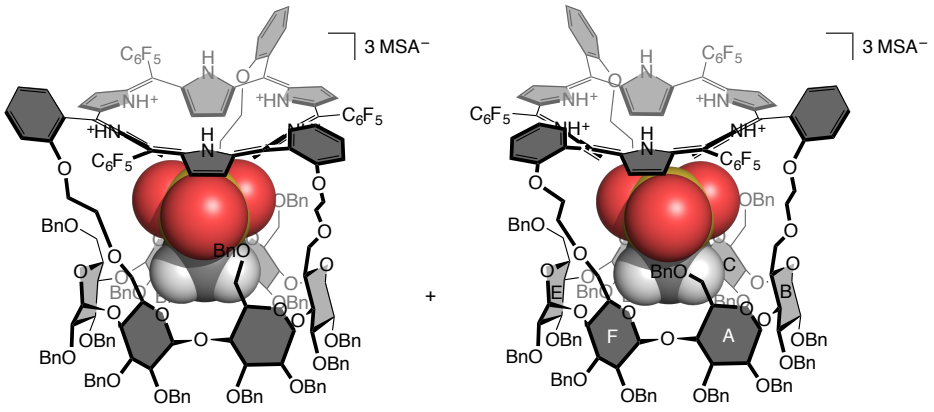

6.1. ^{1}H NMR (600 MHz, CD_2Cl_2, 263 K)

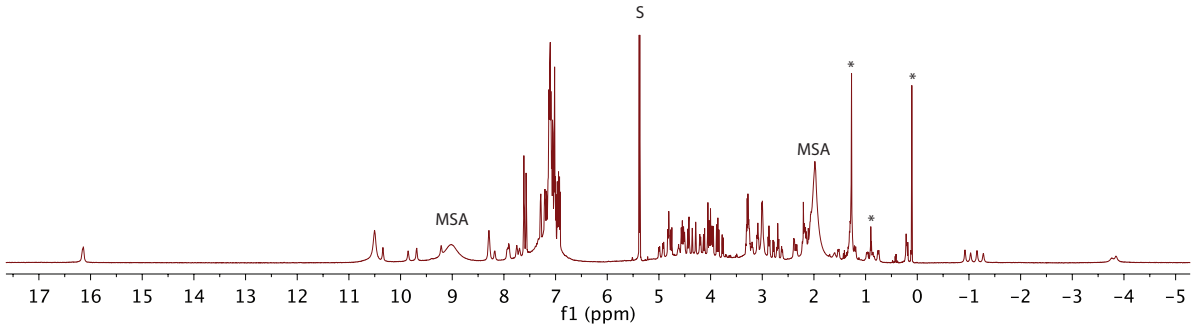

S: solvent and *: impurities.

6.2. ^{19}F NMR (565 MHz, CD_2Cl_2, 263 K)

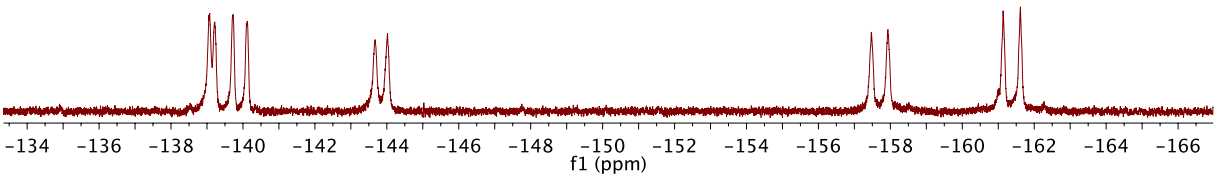

6.3. 2D COSY (600 MHz, CD_2Cl_2, 263 K)

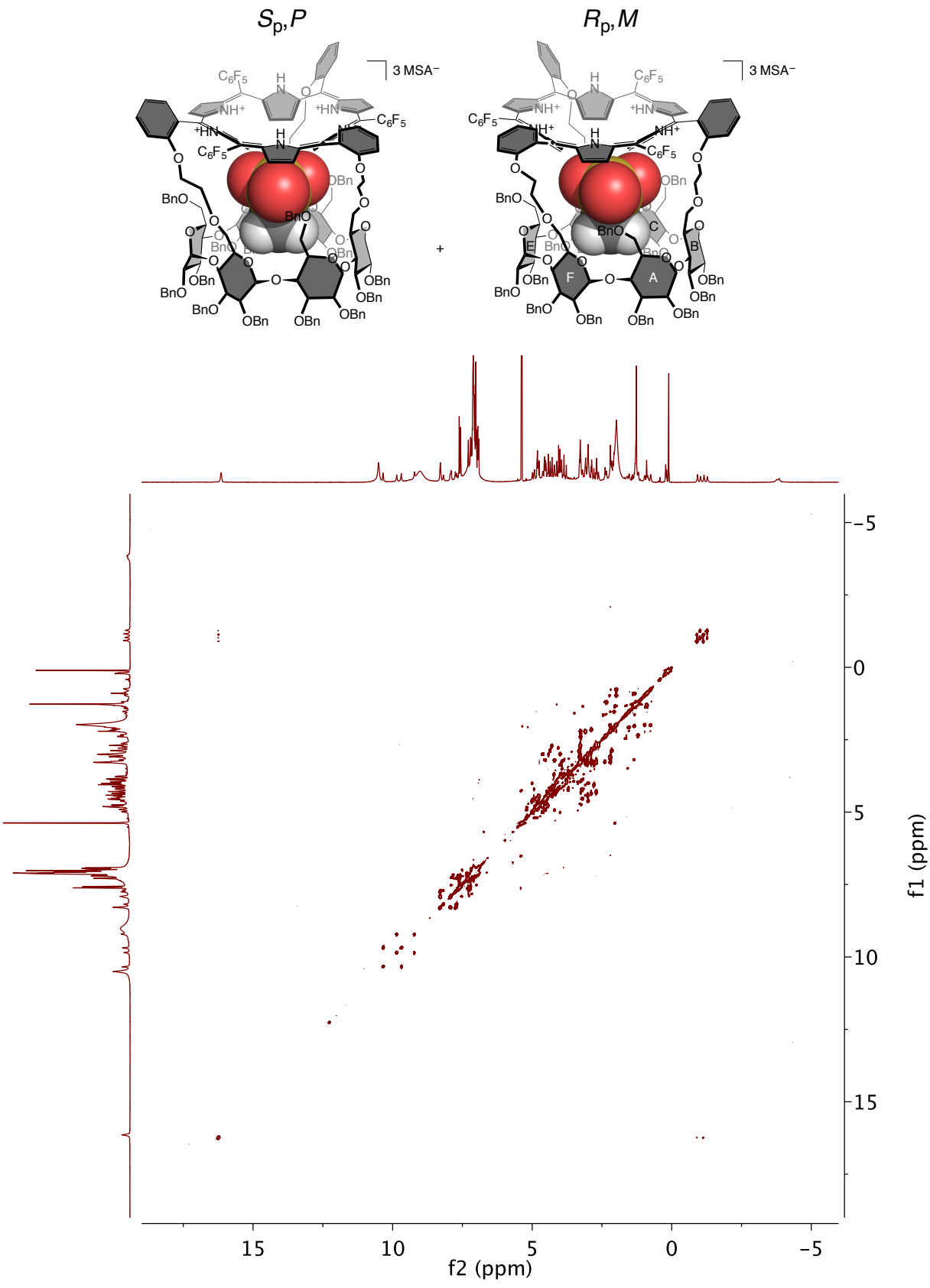

6.4. 2D HSQC-edited (600 MHz, CD_2Cl_2, 263 K)

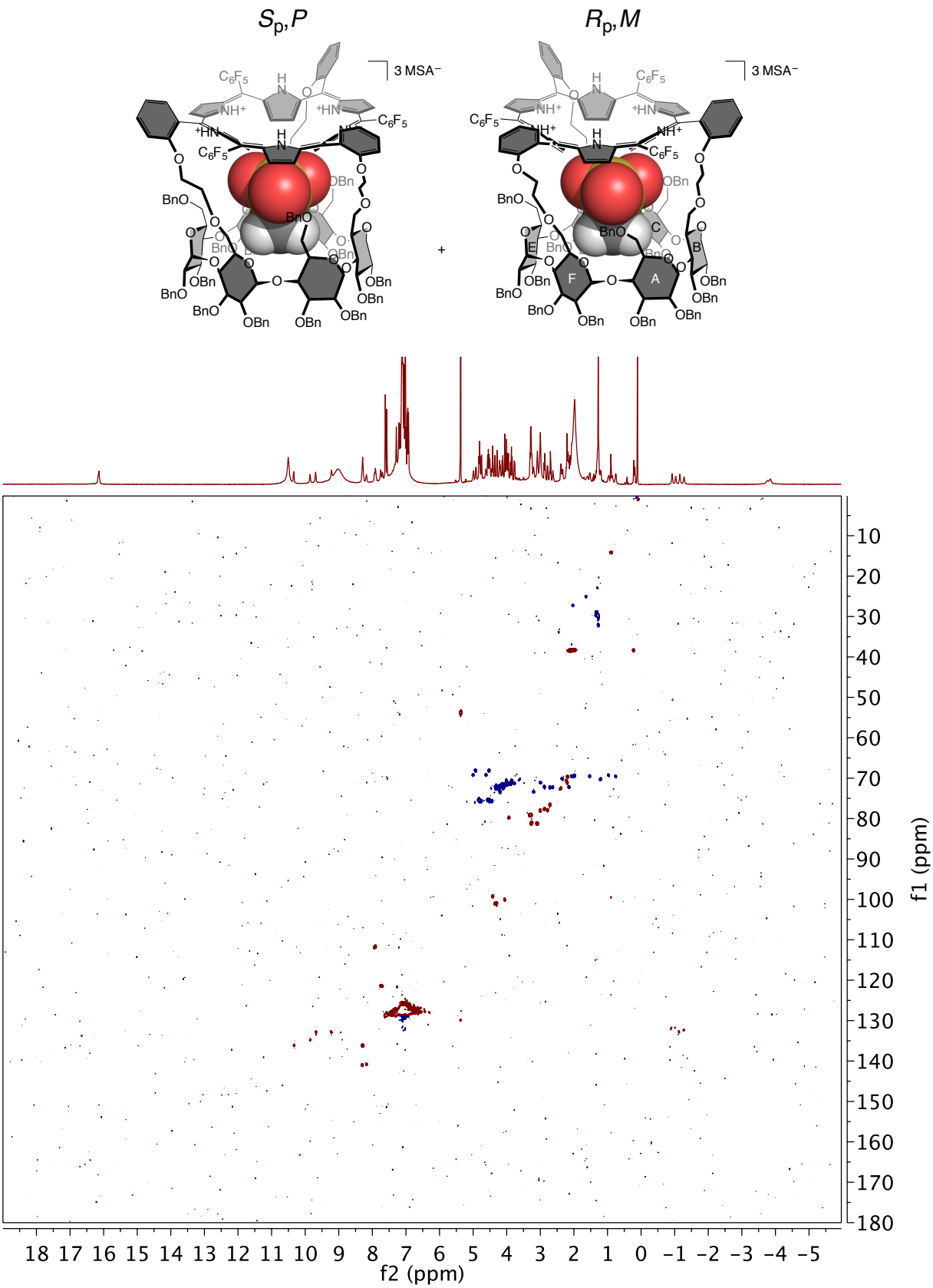

6.5. 2D NOESY (600 MHz, CD_2Cl_2, 263 K, τ = 800 ms)

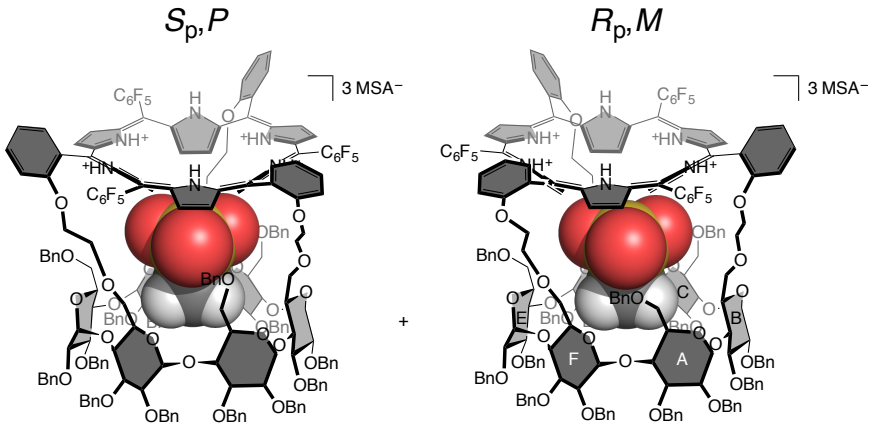

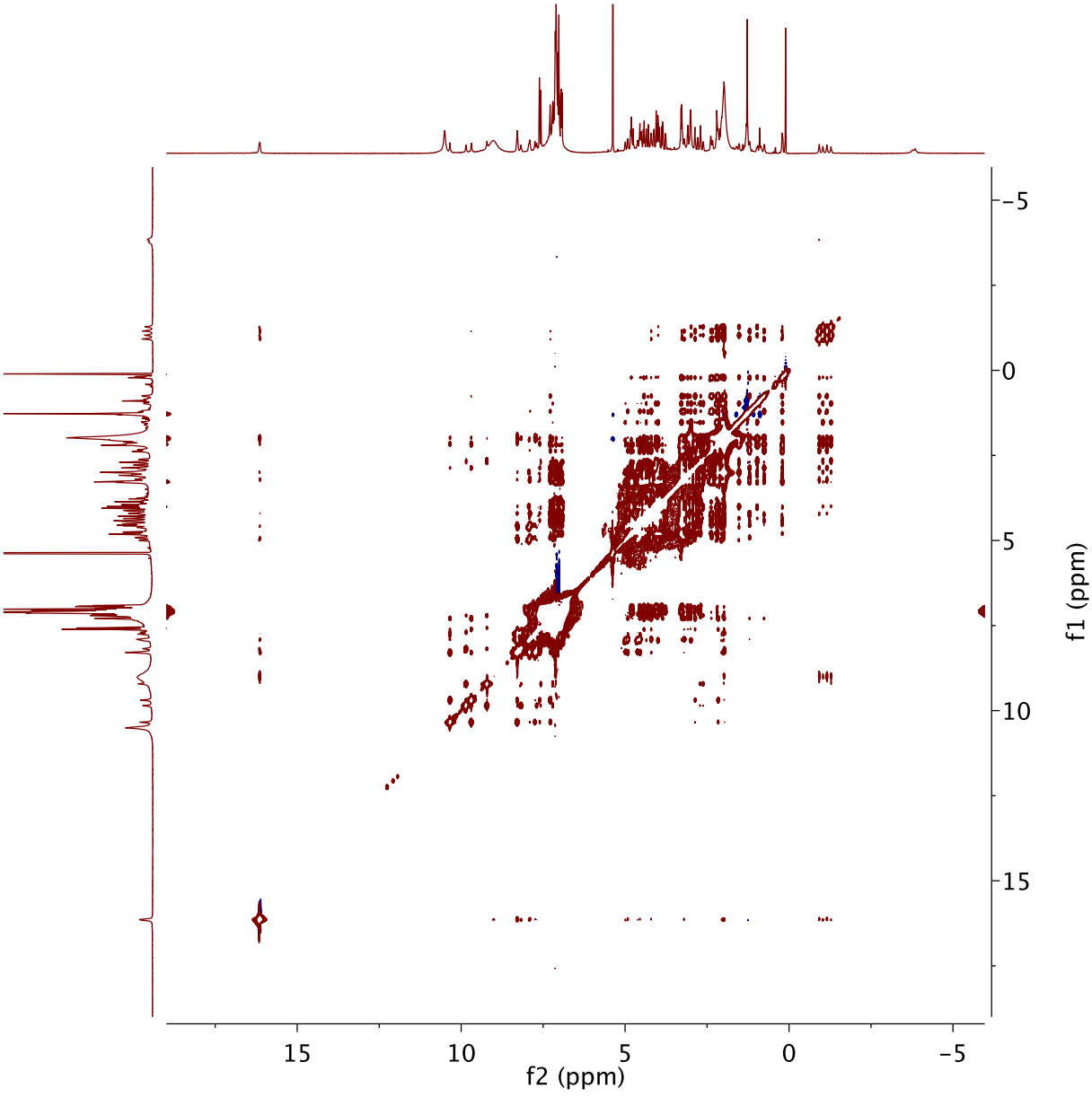

6.6. Zoom on the $\beta\pi_{in}$ correlations region of the 2D NOESY NMR spectrum of ^{T}**[26]HCD•4H^{+}⊃MSA^{-}** (600 MHz, CD_2Cl_2, 263 K)

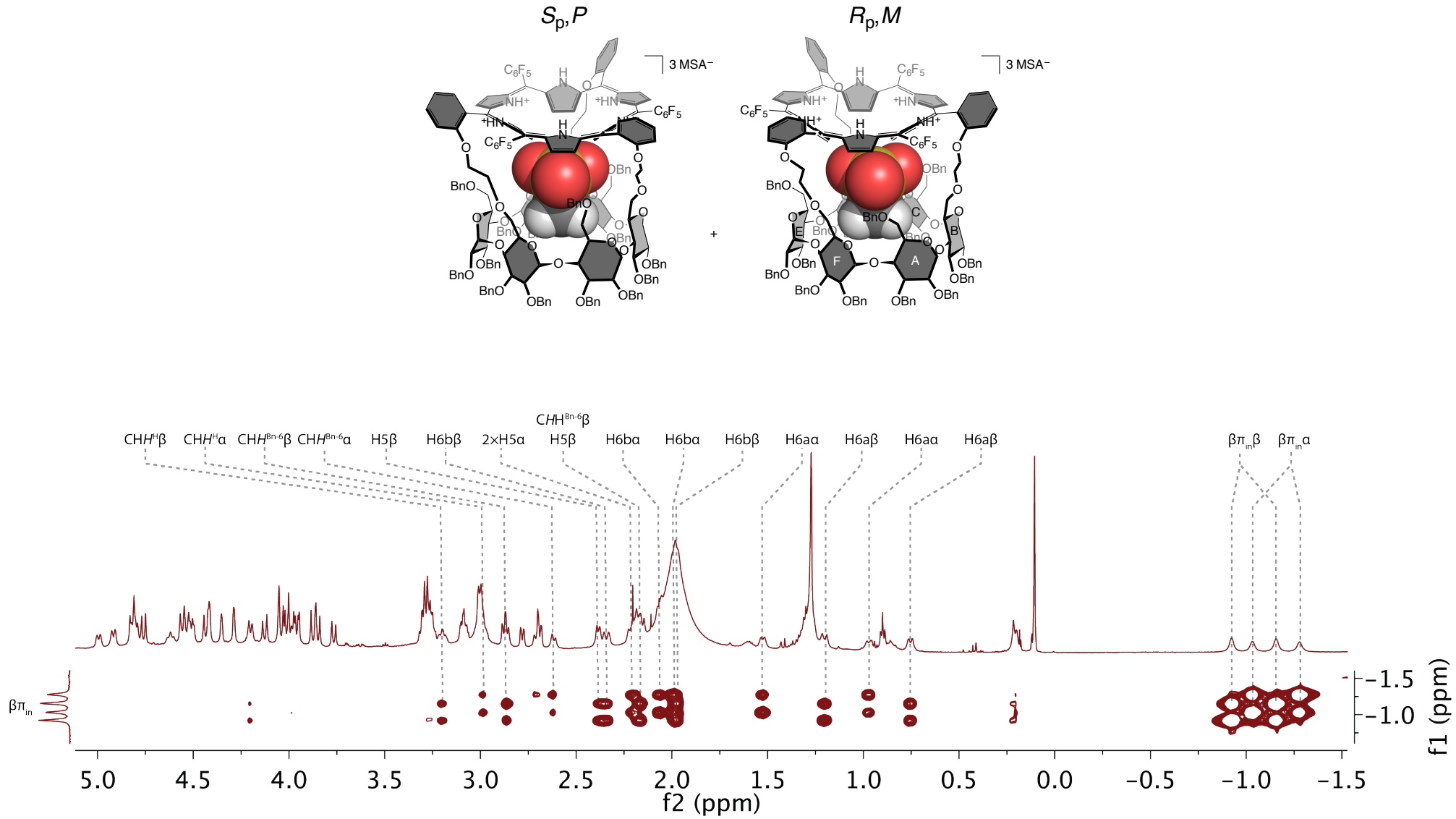

6.7. Zoom on the MSA_{in} correlations region of the 2D NOESY NMR spectrum of ^{T}**[26]HCD•4H^{+}⊃MSA^{-}** (600 MHz, CD_2Cl_2, 263 K)

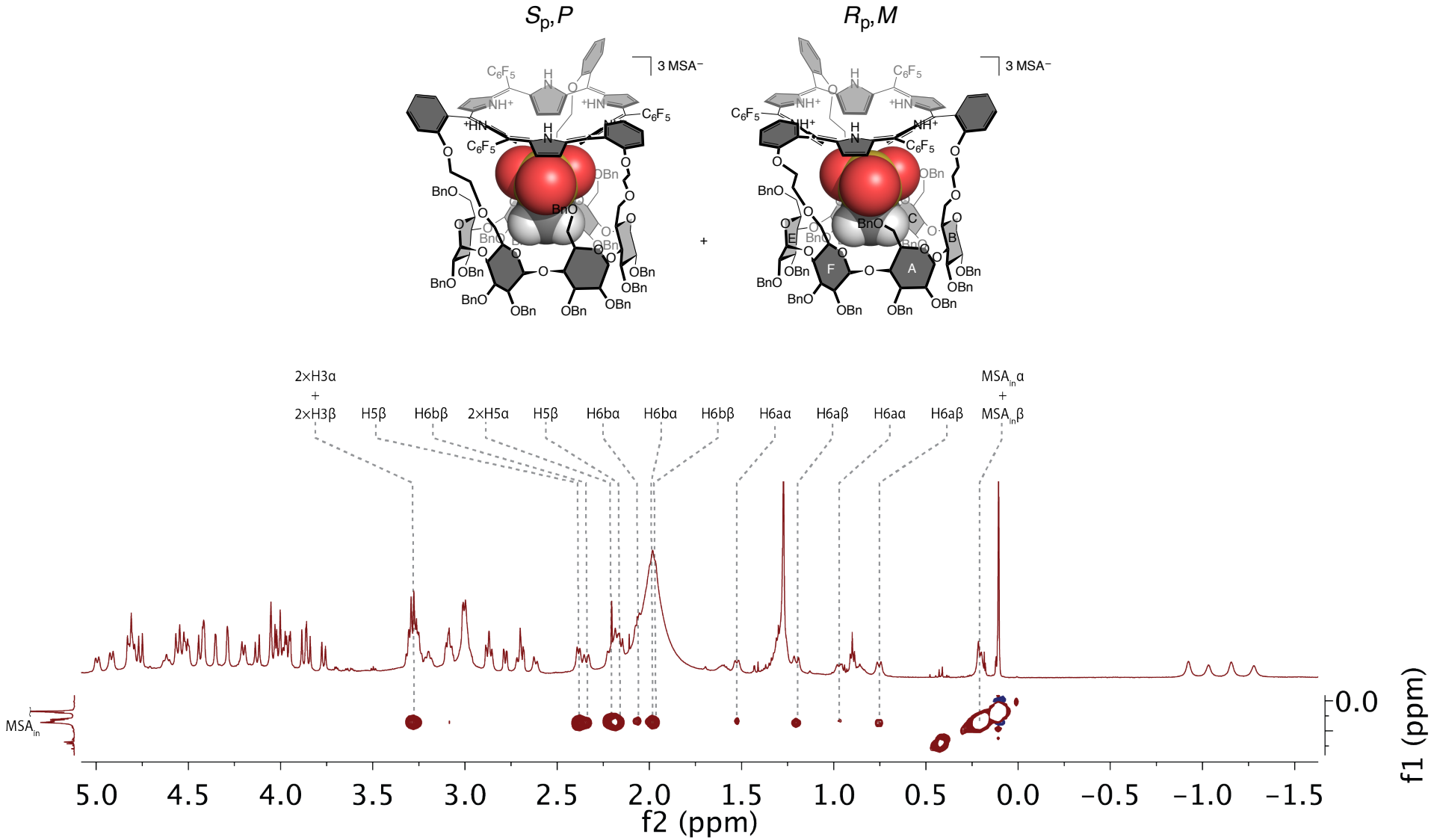

7. NMR spectra of ^{T}**[28]HCD•2H^{+}**

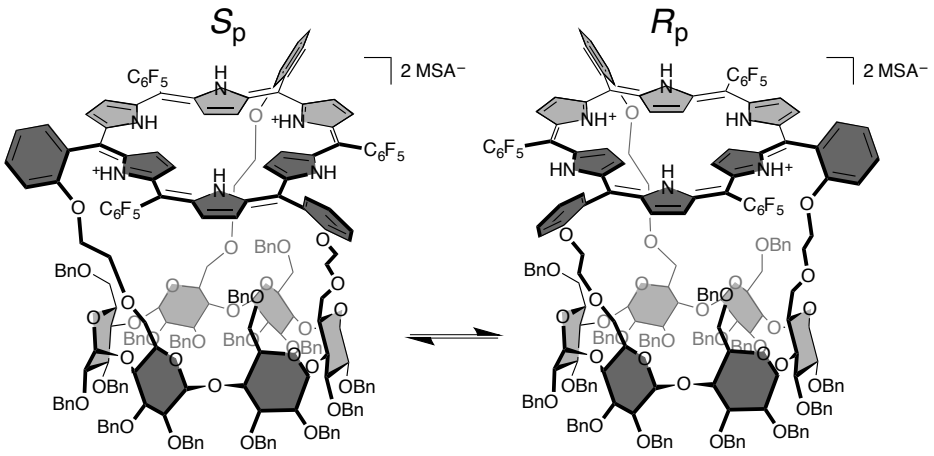

7.1. ^{1}H NMR (600 MHz, CD_2Cl_2, 313 K)

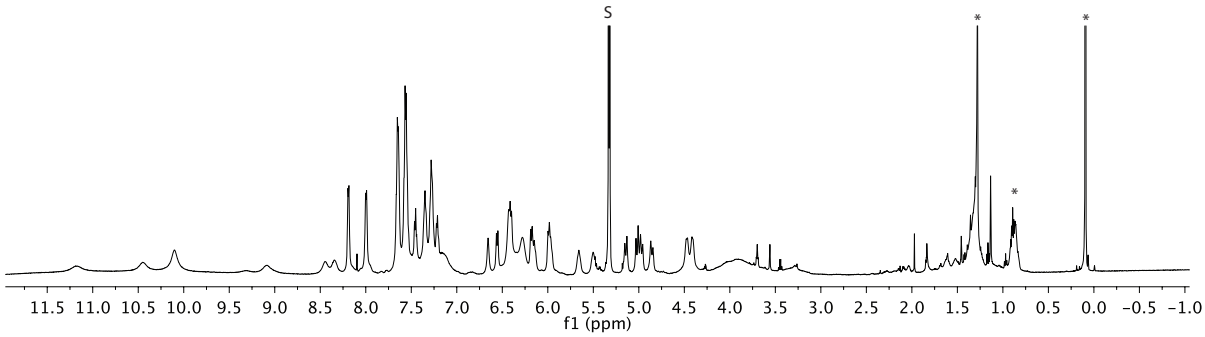

S: solvent and *: impurities.

7.2. 2D COSY (600 MHz, CD_2Cl_2, 323 K)

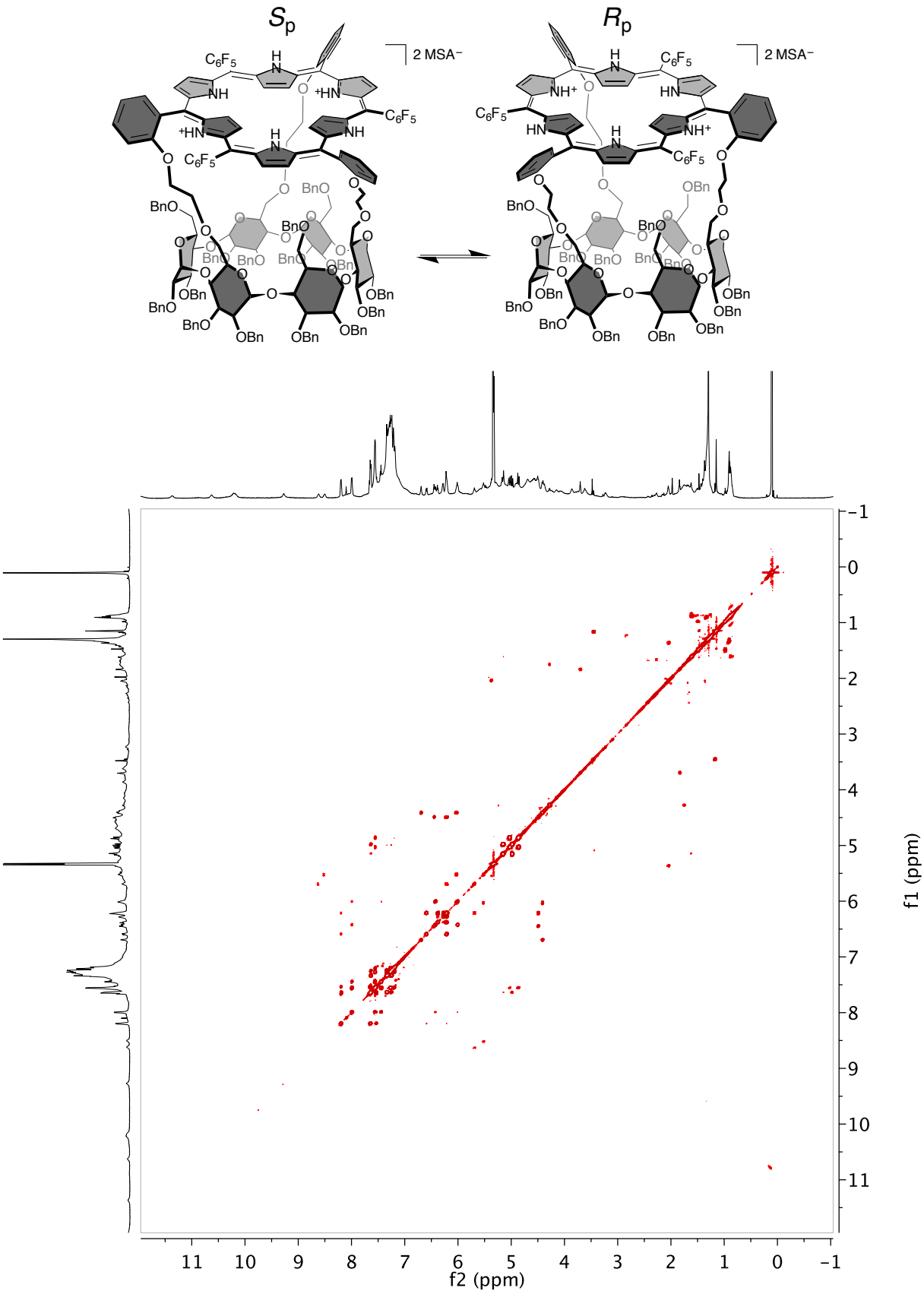

7.3. 2D TOCSY (600 MHz, CD_2Cl_2, 323 K, τ = 240ms)

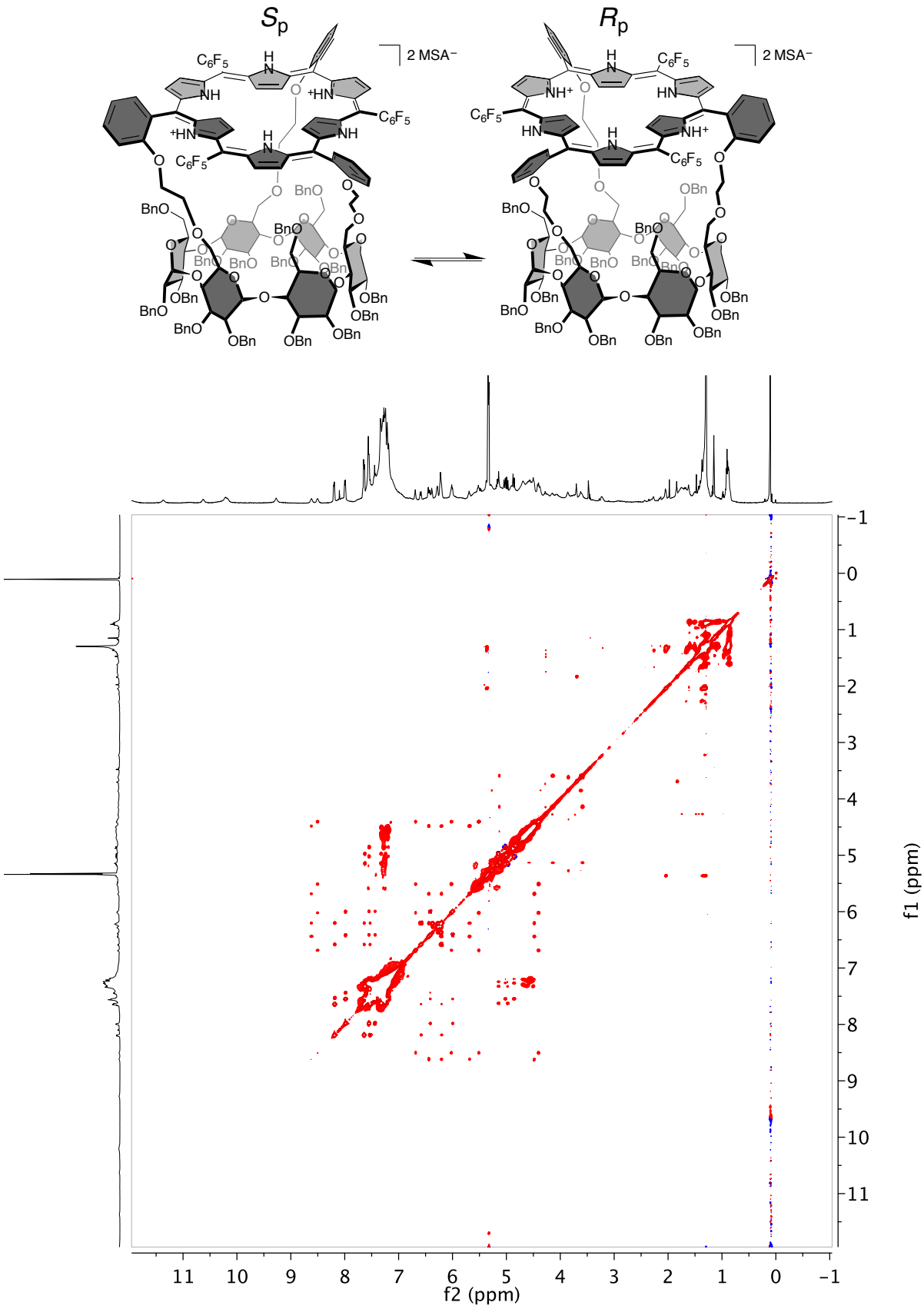

7.4. 2D HSQC-edited (600 MHz, CD_2Cl_2, 313 K)

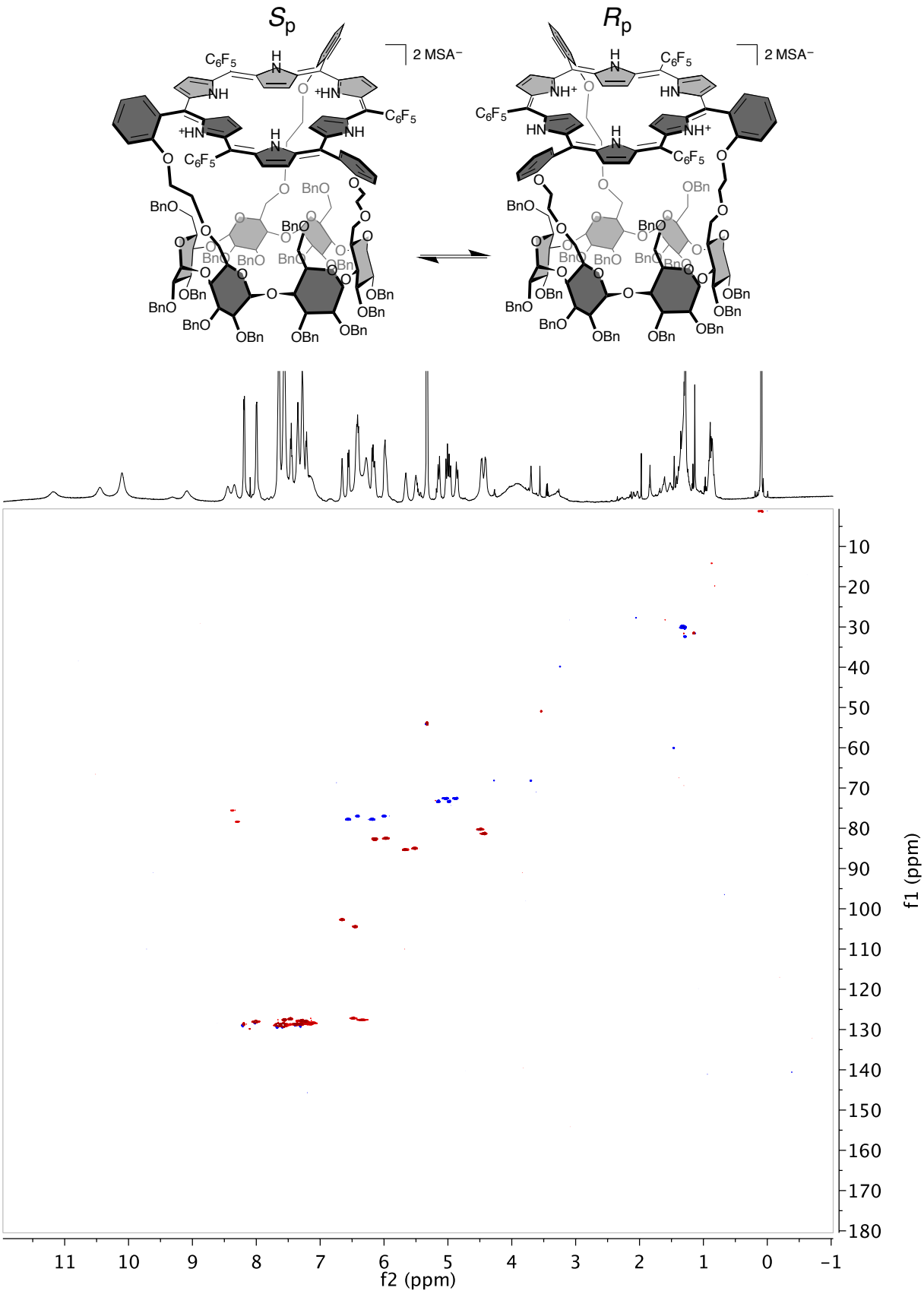

7.5. 2D NOESY (600 MHz, CD_2Cl_2, 313 K, τ = 800 ms)

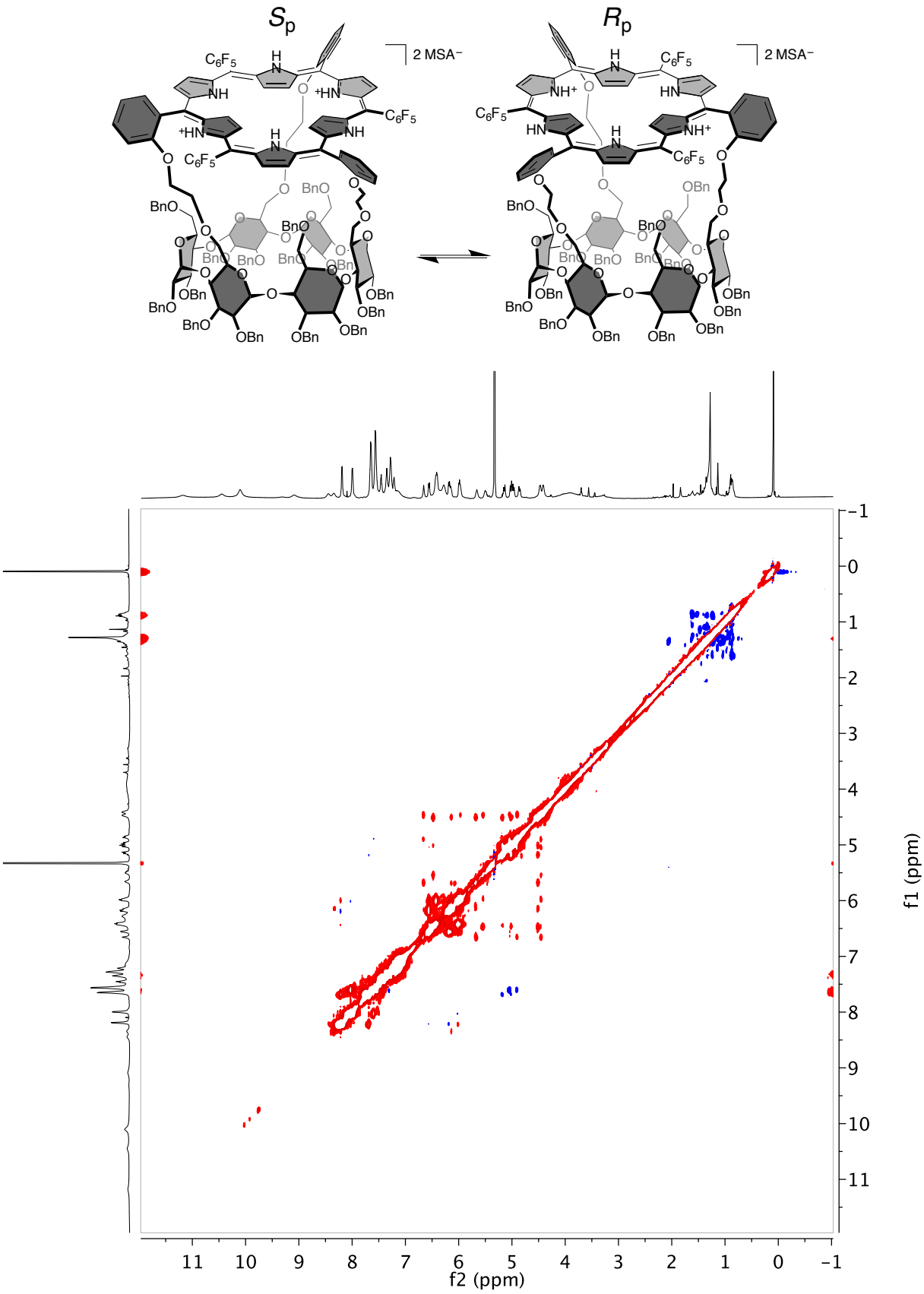

8. Definition of the stereodescriptors related to the inherent planar and "bowl" chiralities in ^{T}**[26]HCD•4H^{+}⊃MSA^{-}**

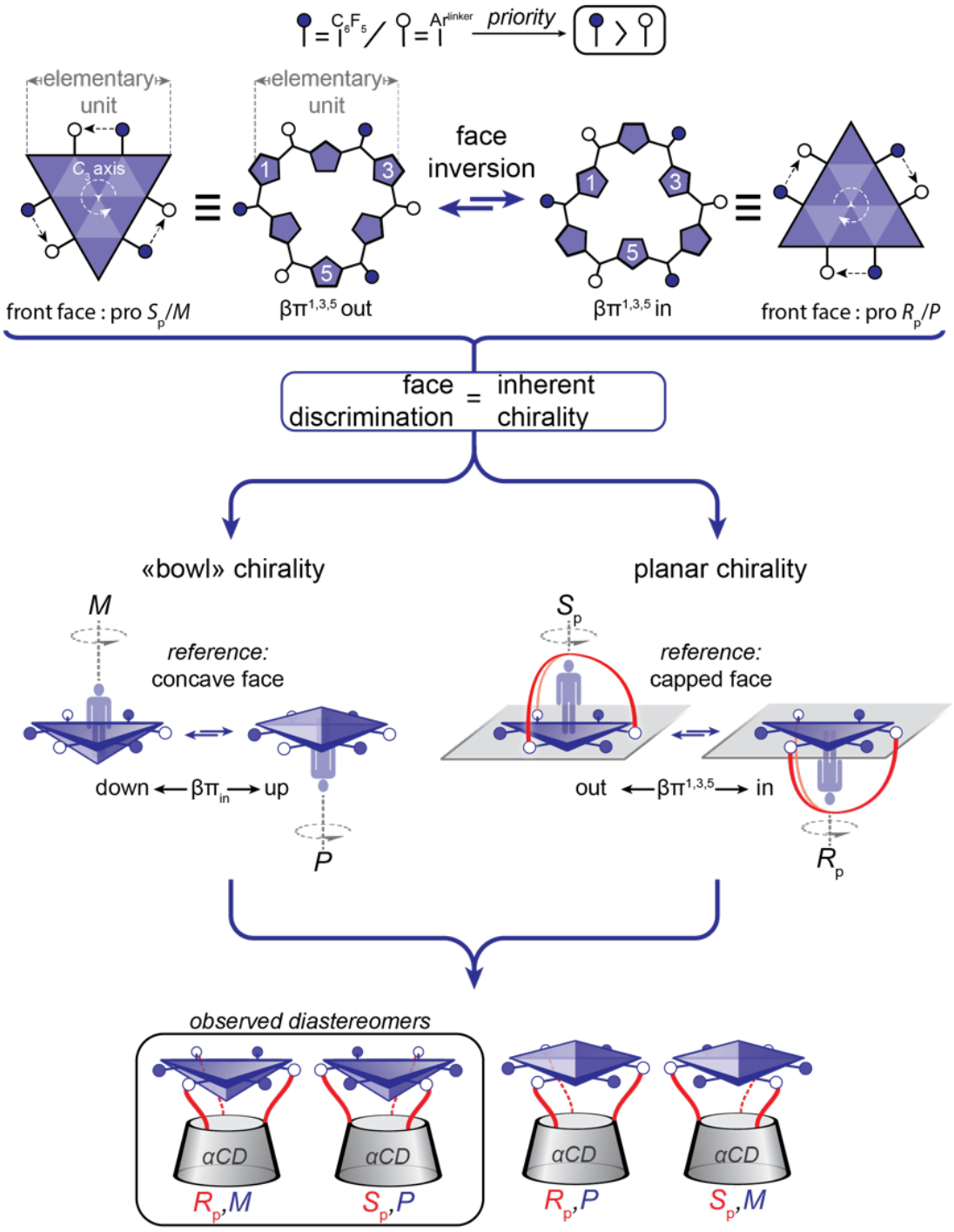

Formally, a triangular planar hexaphyrin can adopt two different $(AB)_3$-type *meso*-substitution patterns, which are dynamically interconvertible through selective *in*/*out* pyrrole inversions. These two patterns are identical when the whole triangle is included within a plane (C_s symmetry), therefore leading to prochiral faces (figure above, top part). However, discrimination of the two faces

induces chirality. In the case of ^{T}**[26]HCD•4H^{+}⊃MSA^{-}**, two types of face discrimination are defining two pairs of stereoisomers, i.e. face capping (planar chirality) and face curvature ("bowl" chirality) (figure above, middle part). These two inherent chiralities are dynamic ones: there is an equilibrium between R_p and S_p enantiomers (planar chirality) through selective *in*/*out* pyrrole inversions (middle part, right), as well as between *M* and *P* enantiomers ("bowl" chirality) through *up*/*down* inner pyrroles tilting (middle part, left). In other words, the faces that are discriminated are interconvertible. Whereas no selectivity is induced by the cyclodextrin unit for the planar chirality (equal amount of R_p and S_p isomers), an impressive selectivity is observed for the bowl chirality, since an inward orientation of the bowl is exclusively obtained. Indeed, the interconversion rate is slow enough to observe two different ^{1}H NMR signatures corresponding to the R_p,*M* and S_p,*P* diastereomers. The stereodescriptors were determined according to the following procedure, although absolute assignment of the NMR patterns was not possible.

- Define the repetitive pattern (the elementary unit)
- Determine the priority of the substituents according to the CIP rules
- Define the reference face (the capped one for planar chirality and the concave one for "bowl" chirality)
- Determine the rotation of the repetitive elementary unit according to the reference face (clockwise : R_p or *P* and counterclockwise S_p or *M*)

9. Comments related to the field effects induced by the protonation of the hexaphyrin

Protonation of the hexaphyrin macrocycle leads to a global aromaticity exaltation enhancing the local field effect illustrated by the chemical shift evolution of the hexaphyrin inner protons. While the aromatic **[26]HCD** undergoes moderate shielding enhancement along the protonation process (Δδ up to -1 ppm, *vide supra*), the antiaromatic **[28]HCD** turns to be highly responsive with Δδ up to +25 ppm (see ***R*[28]HCD•2H$^+$** page 10). In addition, the strongly shifted broad signals at 51 and 39.5 ppm fit the maximum NICS (Nucleus Independent Chemical Shifts) values reported for an ideally planar antiaromatic hexaphyrin (NICS in the range +[40-50] ppm, inner region of the macrocycle)[2] suggesting a similar conformation in the diprotonated state.

[2] J. Sankar, S. Mori, S. Saito, H. Rath, M. Suzuki, Y. Inokuma, H. Shinokubo, K. Suk Kim, Z. S. Yoon, J.-Y. Shin, J. M. Lim, Y. Matsuzaki, O. Matsushita, A. Muranaka, N. Kobayashi, D. Kim and A. Osuka, *J. Am. Chem. Soc.,* 2008, **130**, 13568.